

MTL TR 86-45

AD

DYNAMIC ANALYSIS OF A TACTICAL RIGID SHELTER SUBJECTED TO RAIL IMPACT

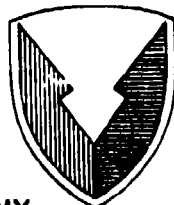
ARTHUR R. JOHNSON
MECHANICS AND STRUCTURES DIVISION

JAMES R. CULLINANE
U.S. ARMY NATICK RESEARCH, DEVELOPMENT AND
ENGINEERING CENTER

December 1986

Approved for public release; distribution unlimited.

DTIC FILE COPY



US ARMY
LABORATORY COMMAND
MATERIALS TECHNOLOGY
LABORATORY

U.S. ARMY MATERIALS TECHNOLOGY LABORATORY
Watertown, Massachusetts 02172-0001

DTIC
ELECTE
JAN 22 1987

A

87 1 21 050

The findings in this report are not to be construed as an official Department of the Army position, unless so designated by other authorized documents.

Mention of any trade names or manufacturers in this report shall not be construed as advertising nor as an official indorsement or approval of such products or companies by the United States Government.

DISPOSITION INSTRUCTIONS

Destroy this report when it is no longer needed.
Do not return it to the originator.

UNCLASSIFIED

SECURITY CLASSIFICATION OF THIS PAGE (When Data Entered)

REPORT DOCUMENTATION PAGE		READ INSTRUCTIONS BEFORE COMPLETING FORM
1. REPORT NUMBER MTL TR 86-45	2. GOVT ACCESSION NO.	3. RECIPIENT'S CATALOG NUMBER
4. TITLE (and Subtitle) DYNAMIC ANALYSIS OF A TACTICAL RIGID SHELTER SUBJECTED TO RAIL IMPACT		5. TYPE OF REPORT & PERIOD COVERED Final Report
		6. PERFORMING ORG. REPORT NUMBER
7. AUTHOR(s) Arthur R. Johnson and James R. Cullinane*		8. CONTRACT OR GRANT NUMBER(s)
9. PERFORMING ORGANIZATION NAME AND ADDRESS U.S. Army Materials Technology Laboratory Watertown, Massachusetts 02172-0001 SLCMT-MSR		10. PROGRAM ELEMENT, PROJECT, TASK AREA & WORK UNIT NUMBERS AMCMS Code: 643726-4280012 D/A Project: 1E463726D428
11. CONTROLLING OFFICE NAME AND ADDRESS U.S. Army Laboratory Command 2800 Powder Mill Road Adelphi, Maryland 20783-1145		12. REPORT DATE December 1986
		13. NUMBER OF PAGES 50
14. MONITORING AGENCY NAME & ADDRESS (if different from Controlling Office)		15. SECURITY CLASS. (of this report) Unclassified
		16. DECLASSIFICATION/DOWNGRADING SCHEDULE
16. DISTRIBUTION STATEMENT (of this Report) Approved for public release; distribution unlimited.		
17. DISTRIBUTION STATEMENT (of the abstract entered in Block 20, if different from Report)		
18. SUPPLEMENTARY NOTES <i>fr. back</i> *U.S. Army Natick Research, Development and Engineering Center, STRNC-UST, Natick, MA		
19. KEY WORDS (Continue on reverse side if necessary and identify by block number) ISO shelters, Dynamic analysis, Shelters Finite element analysis, Tactical shelters Containers Army shelters, Freight containers.		
20. ABSTRACT (Continue on reverse side if necessary and identify by block number) (SEE REVERSE SIDE)		

UNCLASSIFIED

SECURITY CLASSIFICATION OF THIS PAGE (When Data Entered)

Block No. 20

ABSTRACT

→ In this effort a technical database was developed for a Tactical Shelter experiencing rail impact. A finite element model of the shelter and internal equipment was made, a test was conducted in which accelerations were measured on the shelter, the flatcar, and on the internal equipment during rail impact. The measured accelerations on the flatcar were used to determine the spectra of the dynamic loads acting on the shelter and the response of the shelter to forced acceleration impulses in the frequency range of the measured data was determined. We found that the shelter's lowest structural vibration modes, as predicted by the finite element model, were in the range of the frequencies in the power spectral density representation of the rail car response. The shelter responded almost rigidly in the longitudinal direction but did vibrate in the vertical and transverse directions. Computed mode shapes, measured accelerations, analysis of the data and the predicted response of the shelter to impulse loadings are presented in the report.

Keywords:

FLD 19

UNCLASSIFIED

SECURITY CLASSIFICATION OF THIS PAGE (When Data Entered)

PREFACE

The new family of Army Tactical Shelters will be in general use in the near future. The shelters are designed to be made in mass production yet are also intended to be adapted for a variety of missions. The effect of modifications must be determined in the design stage to allow the modified shelters to become available for field use without unjustified development delays. The work reported here represents part of an effort directed towards developing a technical data base on transportation loading environments which the modified shelters must meet.

The authors wish to thank Leonard P. Cuzzupe for helping with the test program and Claudia J. Quigley writing computer programs to process the data.



Accession For	
NTIS STATE	<input checked="" type="checkbox"/>
DTIC TAB	<input type="checkbox"/>
Unannounced	<input type="checkbox"/>
Justification	
By _____	
1. Subject Area	
Availability Codes	
1. 2. 3. 4. 5. 6. 7. 8. 9. 10.	
11. 12. 13. 14. 15. 16. 17. 18. 19. 20.	
21. 22. 23. 24. 25. 26. 27. 28. 29. 30.	
31. 32. 33. 34. 35. 36. 37. 38. 39. 40.	
41. 42. 43. 44. 45. 46. 47. 48. 49. 50.	
51. 52. 53. 54. 55. 56. 57. 58. 59. 60.	
61. 62. 63. 64. 65. 66. 67. 68. 69. 70.	
71. 72. 73. 74. 75. 76. 77. 78. 79. 80.	
81. 82. 83. 84. 85. 86. 87. 88. 89. 90.	
91. 92. 93. 94. 95. 96. 97. 98. 99. 100.	

CONTENTS

	Page
PREFACE.	111
BACKGROUND AND INTRODUCTION.	1
SHELTER AND EQUIPMENT FINITE ELEMENT MODEL	2
FREE VIBRATION MODES OF SHELTER WITH EQUIPMENT INSIDE.	3
ANALYSIS OF TEST DATA.	4
COMPUTED RESPONSE OF SHELTER SUBJECTED TO IMPULSES	9
CONCLUDING REMARKS	9
REFERENCES	10

BACKGROUND AND INTRODUCTION

Army tactical shelters are used in a variety of mission types and must be capable of being easily transported by both military and commercial equipment. The Rail Impact Test is designed to subject a shelter and internal payload to large accelerations which simulate the maximum dynamic loading expected from rail shipment. The test can be briefly described as follows [1]. The shelter is prepared for transportation and an internal payload is added to bring the gross weight of the shelter to 15000 lbs. The shelter is then placed on a 50 ton flatcar and secured with timbers and cables as shown in Figure 1. Two stationary flatcars with their air and handbrakes set are loaded with 50 and 16 tons of rigid payload respectively. The flatcar with the shelter is then brought to a speed of 10 mph, released and allowed to couple with the two stationary cars.

The purpose of this effort is to develop a technical database for Tactical Shelters experiencing rail impact. To do this we: (a) developed a finite element model of a shelter and its internal equipment, (b) conducted a test in which accelerations were measured on the shelter, the flatcar and on the internal equipment during rail impact, (c) used the measured response of the flatcar to determine the spectra of the dynamic loads acting on the shelter and (d) determined the response of the shelter to forced acceleration impulses in the frequency range of the measured data.

A number of finite element models for Army Tactical Shelters have been made. The first model [2] was developed for a prototype three-for-one expandable shelter using the COSMIC*NASTRAN general purpose code. Studies were done during the model development to select a practical mesh for the designers. Due to the poor interpolation of inplane membrane strains as compared to those of the bending strains for the plate elements it was necessary to determine scaling parameters for the inplane stiffness of the shelter panel elements. The design of framework, methods of attaching panels and methods of expanding the shelter were revised in later prototypes. New finite element models were developed [3 & 4] and used as a design tool [4] to indicate how the endwall doors could resist transverse loading of the shelter. The model used for the analysis of transverse loading was upgraded to become a dynamic finite element model of a two-for-one expandable tactical shelter [5]. The upgrade included modeling the nonstructural panels which are used when the shelter is expanded. Low frequency free body vibration modes, the response to a rotational end drop and the response to the Belgian block (spaced bumps) road transportation test were determined. In the rotational end drop test analysis a dynamic load was derived to represent the shelter's interaction with the ground. The load was used directly in the integration scheme. In the Belgian block test analysis a method for enforcing accelerations [6] was used to drive the finite element model's connections to the mobilizers through an acceleration vs time profile which matched the measured response at those points. Computations were made with this model indicating its use as a design tool [5].

In this effort the modeling techniques used to develop the previous tactical shelter finite element models were used again to make a model of a nonexpandable shelter. The latest frame member drawings [7] were used to determine the beam cross section properties. Differences over previous

models include: (a) some of the nodes defining the six walls of the shelter have new locations since that there are no expanding walls and no cargo doors in this model, (b) new section properties and stress recovery points for most beam elements and (c) the internal modular collective protection equipment.

A number of Tactical Shelters have been subjected to the rail impact test. In most cases the tests were of the "pass or fail" type. In 1983 a nonexpandable tactical shelter was instrumented and subjected to a series of rail impact tests [1]. Transient data was collected on 62 channels which included: (a) measuring the forces in the cables, (b) test personnel voice and time channels and (c) accelerations measured using piezoresistive and piezoelectric accelerometers mounted to the shelter and equipment. This test indicated that the shelter was capable of being subjected to the rail impact test without damage but that the equipment inside the shelter during the test may be damaged or even cause minor damage to the interior of the shelter walls and doors. The cable load data obtained was not useable since information on the cable setup (i.e. the tension in the cables, etc.) was not available. The acceleration data indicated that at the corners of the shelter, vertical accelerations near 10g's and longitudinal accelerations near 15-20g's could be expected at the impacted end of the shelter and similar values, but slightly higher, could be expected at the opposite end of the shelter. All the acceleration data was collected on the same time scale. However, the absolute direction in space was not known so the data could not be used to determine natural mode shapes excited. In the effort reported here a second nonexpandable shelter with different equipment inside was tested and analyzed using the finite element method to develop a better understanding of the rail impact test.

In this report we briefly describe the finite element model of the rigid shelter, the natural modes of the shelter below 80 Hz, analyze the test data received and determine the response of the shelter and equipment to a dynamic loading environment similar to that expected during rail impact.

SHELTER AND EQUIPMENT FINITE ELEMENT MODEL

In the transportation mode Tactical Shelters are 8 ft x 8 ft x 20 ft and have corner fittings allowing them to be easily handled. Figure 1 shows the rigid shelter modeled in this effort mounted on a rail flatcar. The finite element (FE) discretization shown in Figure 2 has enough detail to predict the loadings in the major structural elements and the total loadings at the joints. The details of the finite element model made in this effort are similar to those in the model reported in Ref. 4. The equipment and interior walls shown in Figure 3 were also modeled. The equipment and shock mounts were modeled with rigid body and scalar spring elements. Interior walls were modeled with plate and beam elements. Connection of the equipment and interior walls model to the shelter model was made using the multipoint constraint capability in NASTRAN. Figures 4-6 show cross sections of the nonexpandable shelter. All the beams and panels shown were included in the FE model. In addition, the detailed floor frame model given in Ref. 4 was used to model the beams under the floor.

The FE model shown in Figure 2 can be used to obtain the bending response of the beams and panels but not the inplane deformations of the panels (due to the low order inplane interpolation as compared to the bending interpolations). To allow for a reasonable calculation of the overall deformations and load paths in the shelter the inplane stiffness of the panel elements was scaled by a factor of 0.83 (see Ref. 2) to allow these elements to have correct inplane stiffness.

The COSMIC*NASTRAN finite element code was used and a brief description of the elements used is given below:

<u>Element</u>	<u>Description</u>
CBAR	Cubic two node beam element with two bending planes and linear axial and torsional displacements. Used for modeling frame members.
CELAS2	Scalar element which connects two variables in the analysis set. Used to model shock mounts.
CONM2	Elements for mass matrix which allow direct input of the mass and rotational inertia properties of a rigid body. Used to model equipment and shelter corner fittings.
CQUAD1,CTRIA1	Bending, transverse shear and inplane membrane elements. Interpolations are incomplete quintic for bending, linear for transverse shear and linear for membrane. Used for modeling sandwich panels.
CRIGID1,CRIGID2	Rigid link connections of variables in the analysis set. Used to make rigid connections of separately generated meshes such as a wall panel to a roof panel and for connections to shock mounts.

FREE VIBRATION MODES OF SHELTER WITH EQUIPMENT INSIDE

During the FE model development we computed the low frequency free vibration modes of the shelter. With the COSMIC*NASTRAN finite element code one can use the inverse power method to determine all the undamped natural vibration modes in a specified frequency range. The method is not efficient for determining all of the modes in a large frequency range but

is useful for determining all the modes in a narrow range. We used COSMIC*NASTRAN and successively selected frequency ranges starting with a narrow range near zero to determine the modes listed in Table 1.

A modeling problem was surfaced by the eigenvalue extractor. At first we were unable to obtain the rigid body modes. Having previously determined these modes for the shelter model without the internal equipment and walls we reviewed the constraint relationships which connect the new sections of the structure together, the rigid body equipment models and the shock mount models. The scalar elements modeling the shock mounts caused the loss of rigid body modes. Scalar elements should not be connected between nodes with different locations in a structural model. These elements do not carry the geometric information necessary to retain rigid body modes. In a linear structural analysis the scalar elements can only be connected between overlaid nodes. We modified the shock mount models to reflect the above requirement and obtained the structure rigid body modes.

Plots of the mode shapes indicated that up to about 20 Hz the nonzero modes consisted of rigid body shelter - equipment vibrations, see Table 1. One of the modes was approximately a rotation of the gas particulate fan unit (GPFU) about its own z - axis (the axis parallel to the global z - axis.) The computed frequency was 46.58 HZ which includes the effects of the shelter. Considering the shelter as a rigid support for the GPFU and using the data input to the finite element program we calculated, by hand, a frequency of 46.66 Hz for this mode. This computation along with the six zero frequencies for the rigid body modes helped facilitate model verification.

The mode shapes corresponding to the frequencies over 30 Hz consisted of combinations of structural deformations of the shelter mixed with motions of the equipment. At the higher modes (over 45 Hz with one exception) the mode shapes were mainly structural deformations. Figures 7 through 16 show some of the mode shapes in which the walls, roof and floor of the shelter are active for the frequency range from 34 Hz to over 70 Hz. The mode shown in Figure 7 shows the protective entrance wall moving transversely and upward to the left. This motion appears inconsistent with the motion of the roof, floor and curb sidewall. However, the connection between the protective entrance wall and the more rigid panels is through a slip joint which contains the wall in the longitudinal direction. Small transverse deformations of this interior wall are allowed and the mode shape is correct. The modes shown in Figures 8 through 10 show many areas of the structure active and indicate that the roof may be excited by vertical dynamic forces in the frequency range from 45 Hz to 50 Hz. Similarly, longitudinal modes for the endwalls and doors may also be excited in this frequency range. The mode shapes for frequencies above 60 Hz appear to consist of complex deformations of the panels.

ANALYSIS OF TEST DATA

The rail impact tests were conducted by the Combat Systems Test Activity (CSTA) at Aberdeen Proving Ground, MD during December 1984 on a Chemical/Biological (CB) Non-Expandable ISO Army Shelter. In the tests accelerometers were mounted on the shelter, Environmental Control Unit

Table 1. LOWEST UNDAMPED NATURAL MODE FREQUENCIES AND COMMENTS ON
AREAS OF THE SHELTER CONTRIBUTING TO THE MODE SHAPES

Mode No.	Frequency Hz	Comment on Mode Shape
1-6	0.00000	Rigid body modes
7	8.51526	Environmental Control Unit (ECU), Gas Particulate Fan Unit (GPFU), and rigid motion of shelter
8	10.50432	"
9	12.19836	"
10	12.55025	"
11	16.06804	GPFU
12	18.51087	ECU
13	19.82533	ECU
14	20.81366	ECU
15	23.74194	Interior door (mode 1)
16	30.84827	Interior door (mode 2)
17	31.62459	Interior door, GPFU, ECU
18	34.14961	Roof and interior walls
19	45.8257	Entire structure
20	46.58091	GPFU
21	48.58676	Roof and sidewalls
22	49.13905	Entire structure
23	49.98732	Protective entrance wall
24	60.18068	"
25	64.04985	"
26	67.244443	All walls and roof
27	67.49761	Higher order modes of roof and walls
28	69.18818	Interior walls
29	71.33157	Higher order modes of roof, floor and walls
30	71.77115	"
31	71.90845	"
32	74.41150	GPFU
33	78.13871	Higher order modes of structure
34	79.88224	"
35	80.54820	"
36	81.38745	"
37	82.20754	Higher order modes of interior walls

(ECU), Gas-Particulate Filter Unit (GPFU) and on the rail car near the cable tie-down fittings. For a detailed description of the test see Reference 8. In this section we present acceleration data from test #8. The signals have been filtered to the range 0-100 Hz but power spectral density analyses indicated that there is no significant contribution to the acceleration data from harmonics with frequencies in the range 100-200 Hz. In test #8 the end of the rail car corresponding to the front end of the shelter was the impact end and the speed at impact was 9 mph. There was no payload in the shelter.

Longitudinal acceleration profiles are shown in Figures 17-23. The accelerations along the road side of the rail car (Figure 17) have peak values between 40 and 50 g's. The pulse shape at the rear of the rail car is more complex than those at the front or center of the car. The profiles along the road side wall (Figure 18) are smooth in shape and also have peaks in the range 40 to 50 g's. The smooth shape suggests that the shelter - rail car interface filters out some of the high frequency railcar response. The floor (Figure 19) responded with low peak values (20 g's) indicating either an error in recording or processing the data or that the floor is responding drastically differently than the rail car and the side wall. The roof's maximum longitudinal acceleration was approximately 30 g's (Figure 20) which is higher than the floor's but lower than the side wall's accelerations. Accelerations at the bottom and top of the sidewalls near the rear of the shelter are shown in Figures 21 and 22. It appears that the road side wall accelerations are slightly smaller in magnitude than the curb side wall accelerations. That is, the measured data indicated that the response was not completely symmetric. Data at the top of the curb side wall near the front of the shelter (Figure 23) was not similar to the data near the rear of the shelter (Figure 22).

Profiles of the vertical accelerations are shown in Figures 24 - 28. These accelerations are of much lower magnitude than the longitudinal accelerations. The rail car data (Figure 24) contains more high frequency content than the shelter data (Figures 25 - 28) which again indicates that all the high frequency motion of the rail car does not transmit to the shelter. In general, the magnitude of the accelerations are on the order of 10 g's.

The acceleration profile shown in Figure 29 was taken from the top of Figure 28. The curve has the appearance of a damped harmonic response. Since it represents the motion at a point which could measure "drum head" response (mode 1) of the roof we studied the data in more detail. Working from graphs we read uniformly spaced acceleration vs time data (a,t) by hand. The reconstructed curve is shown as "input data" in the center graph on Figure 29. We then fit the measured data to a damped harmonic using a simple nonlinear least squares curve fit as follows.

$$\text{Let} \quad A(t_i) = C e^{-\zeta t_i} \sin(\omega t_i) \quad (1)$$

represent the damped harmonic approximation to the data at t_i . Then find C, ζ and ω such that

$$F = \sum_{i=1}^N [a(t_i) - A(t_i)]^2 \quad (2)$$

is minimized where

$a(t_i)$ = the measured acceleration data at t_i .

To do this we used the Newton-Raphson method where the update is given by

$$\begin{bmatrix} C \\ \zeta \\ \omega \end{bmatrix}_{\text{new}} = \begin{bmatrix} C \\ \zeta \\ \omega \end{bmatrix}_{\text{old}} - [K]_{\text{old}}^{-1} [g]_{\text{old}} \quad (3)$$

where $[g] = \begin{bmatrix} \frac{\partial F}{\partial C} \\ \frac{\partial F}{\partial \zeta} \\ \frac{\partial F}{\partial \omega} \end{bmatrix} \quad (4)$

$$[K] = \begin{bmatrix} \frac{\partial^2 F}{\partial C^2} & \frac{\partial^2 F}{\partial C \partial \zeta} & \frac{\partial^2 F}{\partial C \partial \omega} \\ & \frac{\partial^2 F}{\partial \zeta^2} & \frac{\partial^2 F}{\partial \zeta \partial \omega} \\ & & \frac{\partial^2 F}{\partial \omega^2} \end{bmatrix} \quad (5)$$

(sym)

The result of the curve fit is shown in the center graph of Figure 29. We found

$$A(t) = 19.983 e^{-23.257 t} \sin(213.06 t) \quad (6)$$

Making an analogy to a damped single degree of freedom system we have the undamped frequency as

$$f = 34.1 \text{ Hz}$$

and $\zeta = 0.108$ as the damping coefficient.

This frequency corresponds to the frequency of the first structural mode (Figure 7). However, the mode shape for the first mode does not indicate significant vertical motion of the roof near the front of the shelter. The first undamped vibration mode of the shelter, which has the roof in a drum head shape, is predicted by the finite element model to be at $f = 45.8 \text{ Hz}$ (Figure 8). This suggests that the stiffness and/or inertial modeling is in error in the finite element code.

The total signal is made up of many harmonics. To measure the contribution of the least squares fit, eq (6), to the total signal, we computed Fast Fourier Transforms of both the original signal and of the original signal minus the least squares fit. We then computed the corresponding power spectral densities. The results are shown in the bottom of Figure 29. The power spectral density (PSD) graph indicates that the original data can be represented with signals from the range of 20 to 40 Hz and that if the single damped harmonic of equation (6) is removed the PSD curve is significantly flattened. Thus, point 101 on the front roof was vibrating in the vertical direction like a damped harmonic oscillator. This suggests that the first drum head mode of the roof occurs at a lower frequency than the finite element model predicts. Note, the other accelerometer at the location 104 on the roof was near to being over the interior wall. As a result, gauge 104 was near a node of the first drum head mode (see Figure 7) and responded differently than gauge 101.

Most of the longitudinal acceleration versus time profiles have similar shapes (Figures 17 to 23). At the bottom of Figure 30 a typical longitudinal acceleration profile is shown. It is desirable to determine how the pulse shape is related to the test setup of the rail cars. To do this we modeled the three rail cars as shown at the top of Figure 30. Using Reference 9 (Chapter 45 on Rail Vehicles) we estimated the stiffness of the draft gears between the flat cars. According to Reference 9 each gear should be capable of absorbing 80,000 ft-lbs of energy in 4-3/4 inches of stroke without exceeding 0.5×10^6 lbs force on the flatcar. Using these numbers and numerous variations of the resisting frictional forces of the two stationary cars we analyzed the nonlinear system shown (nonlinear because of the static and kinetic friction). We were unable to predict large accelerations (40 g's) for any values of the draft gear stiffness and a reasonable values for the friction coefficients. We then used the nonlinear draft gear stiffness shown in the center of Figure 30. With this model we were able to predict the steep climb and amplitude of the pulse. Our prediction of the climb and maximum value is plotted at the origin of the bottom graph in Figure 30. Further study of the literature on high energy shock absorbers [10] indicated that these absorbers have a resistance curve similar to the measured longitudinal acceleration curves.

We selected one longitudinal curve and two vertical curves for further study. In Figure 31 the longitudinal acceleration at the midfront road side wall (location 303 in Figure 18) is shown. A "window" of the data was approximated as shown in the center graph. The PSD curve for the windowed data is shown in the bottom graph. It indicates that the frequency content of the pulse is below 40 Hz. Considering that the vibration modes predicted by the finite element model indicate no significant longitudinal deformations below 48.5 Hz it is likely that the shelter responds rigidly in the longitudinal direction during rail impact. The vertical pulses shown in Figures 32 and 33 and their PSD curves (see Figure 25 for locations) indicate response in the frequency range of structural modes.

The above analysis of the data and the finite element model calculations suggest the following. During rail impact the shelter will respond rigidly in the longitudinal direction (except for the endwalls). The roof, side walls and floor will deform out of plane as a result of vertical excitation from the rail car. Although high frequency

accelerations (over 100 Hz) will be part of the general motion of the shelter the PSD curves indicate that most of the energy is passed by harmonic components under 100 Hz.

COMPUTED RESPONSE OF SHELTER SUBJECTED TO IMPULSES

After the finite element model was completed and the PSD curves were available for the measured accelerations [8] we computed the response of the shelter to impulse loadings. Since most of the energy is transferred to the shelter in the frequency range of 0 to 100 Hz we selected impulse loadings which would have an application time equivalent to 25, 50 and 75 Hz harmonics. The shapes of the impulse loadings were triangular with rounded tops. We computed the response of the shelter and internal equipment for each impulse. The locations of the impulse loads and output accelerations are shown in Figure 34. The results for the vertical impulses are shown in Figure 35. We plotted vertical accelerations only. It can be seen that low frequency harmonics in the vertical input load spectrum (25 Hz impulse) cause slightly larger accelerations in the roof and for the GPFU, while a lower acceleration amplitude is experienced by the ECU. For 50 and 75 Hz impulses the equipment experiences delayed but lower accelerations. The roof accelerations are delayed with respect to, but have similar amplitude as, the input. The results for the longitudinal impulses are shown in Figure 36. We plotted longitudinal accelerations only. Here the center of the roof responds the same as the top of the corner post. The finite element model predicts a slight delay in the response of the roof with respect to the input at the floor. However, for design purposes, the top and bottom of the shelter respond almost identically in the longitudinal direction. The equipment responds slower (out of phase) and with reduced amplitude.

When designing equipment shock mounts for rail impact, the shelter / equipment / shock mount system should be modeled and the system response determined as shown in Figures 35 and 36. The finite element output will contain approximate shock mount loads and the information needed to estimate the maximum acceleration levels experienced by the equipment.

CONCLUDING REMARKS

A data base for rigid tactical shelters experiencing rail impact has been developed in this effort. The data base consists of plots of measured accelerations on the rail car and on the shelter for several tests, the analysis of the data for test #8 and the comparison of that test data to the structural dynamic characteristics of the shelter predicted by the finite element model. We found that the shelter's lowest structural vibration modes, as predicted by the FE model, were in the range of the frequencies in the power spectral density representation of the rail car response. However, the longitudinal dynamic loading imposed by the rail car is unlikely to excite many modes of the shelter. That is, the shelter will respond almost rigidly to the longitudinal dynamic load imposed by the rail car. The vertical excitations will excite natural modes of the shelter which involve the roof and walls bending out of plane. The longitudinal accelerations, being two-to-four times larger than the vertical accelerations and dictated by the design of the draft gear on the

rail car, indicates that an important consideration in rail shipping of shelters is having the knowledge of the class of rail cars on which the shelters are shipped.

REFERENCES

1. W. C. Brown, "Rail Impact Testing of Nonexpandable ISO Shelter Equipped with ECU", Aberdeen Proving Ground Report No. APG-MT-5895, September 1983.
2. A. R. Johnson and V. P. Ciras, "Finite Element Analysis of a Statically Loaded ISO Tactical Shelter", Technical Report NATICK/TR-79/023, US Army Natick Research and Development Command, Natick, MA 1979 (AD-A075808).
3. D. E. Johnston, "Structural Analysis for a One-Side Expandable ISO Tactical Shelter", Contractor Report No. DAAK-60-78-C-0011, Brunswick Corp., Defense Division, Marion, VA, February 1979.
4. A. R. Johnson, "Response of a Two-for-One Tactical Shelter to Racking Loads", Technical Report NATICK/TR-81/016, US Army Natick Research and Development Laboratories, Natick MA, 1981 (AD-A102389).
5. A. R. Johnson, "Analysis of Accelerations in a Dynamically Loaded Tactical Shelter", Technical Report NATICK/TR-83/007, US Army Natick Research and Development Laboratories, Natick, MA, 1982 (AD-A124378).
6. J. A. Joseph, editor, "MSC/NASTRAN Application Manual for CDC 6000 Series", Section 2.7, MacNeal-Schwendler Corp., 1972.
7. "Shelter Configuration Drawing List", FSCM No. 81337 Drawing No. 5-4-2789 dated August 26, 1982, US Army Natick Research and Development Laboratories, Natick, MA.
8. L. G. Stepnitz, "Engineer Design Test of Nonexpandable ISO EMI Shelter", USACSTA-6159, Aberdeen Proving Ground, MD 21005-5057, February 1985.
9. C. K. Harris and C. E. Crede, Shock and Vibration Handbook, McGraw-Hill Book Co., 1961.
10. N. P. Chironis, Spring Design and Application, McGraw-Hill Book Co., 1961.

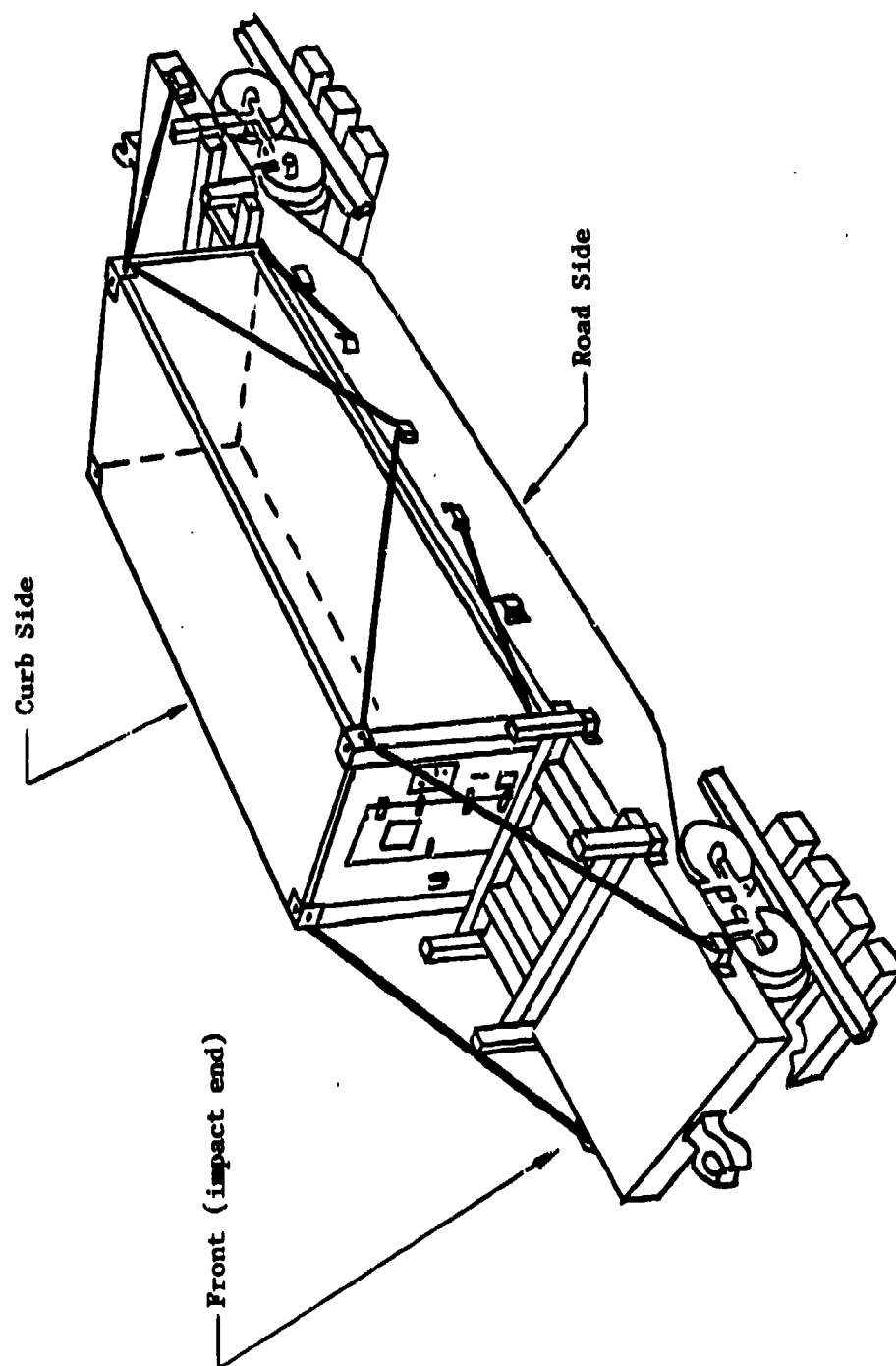


Figure 1. Tactical Rigid Shelter blocked and tied down on a railroad flatcar.

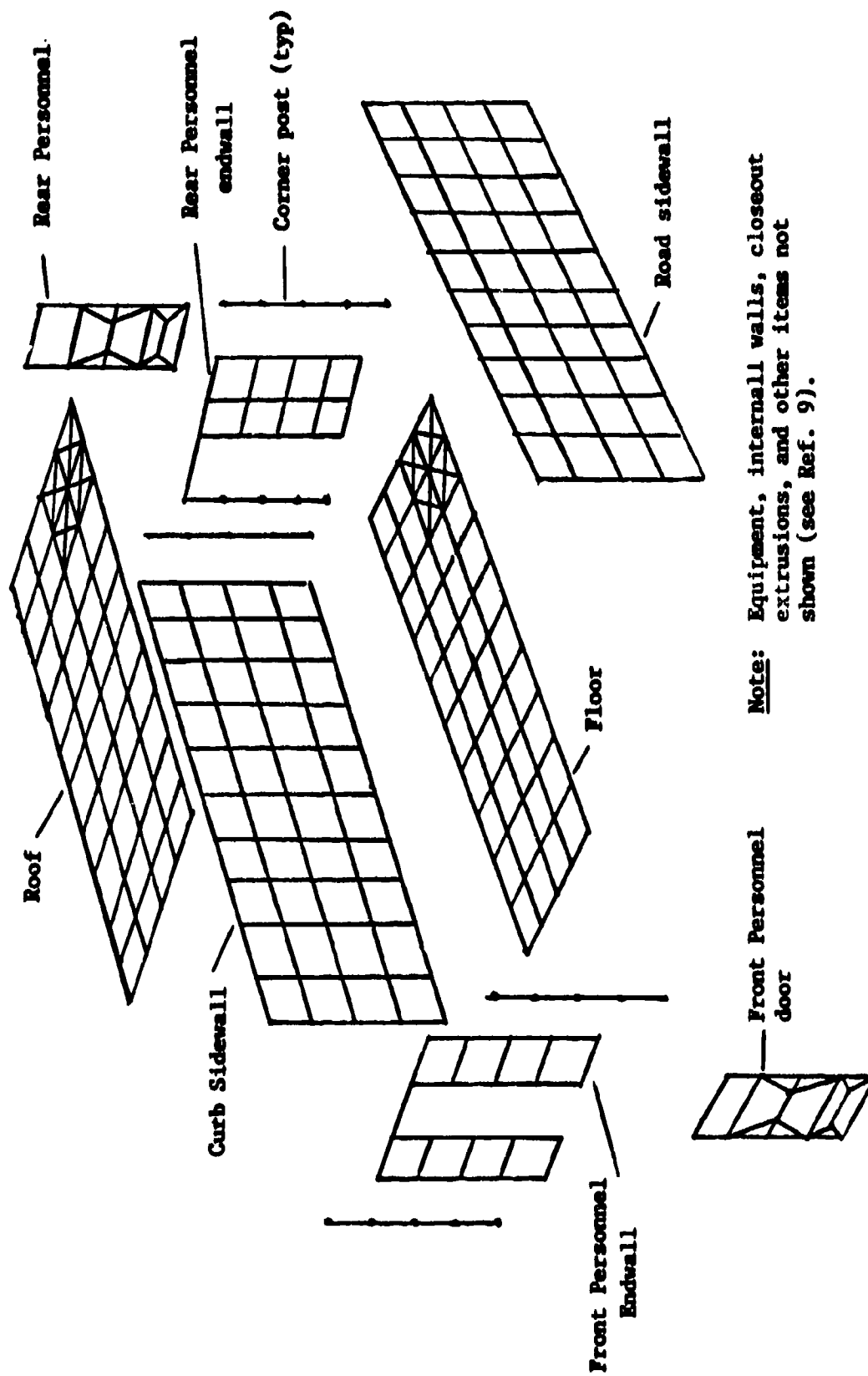


Figure 2. Finite Element discretization of shelter.

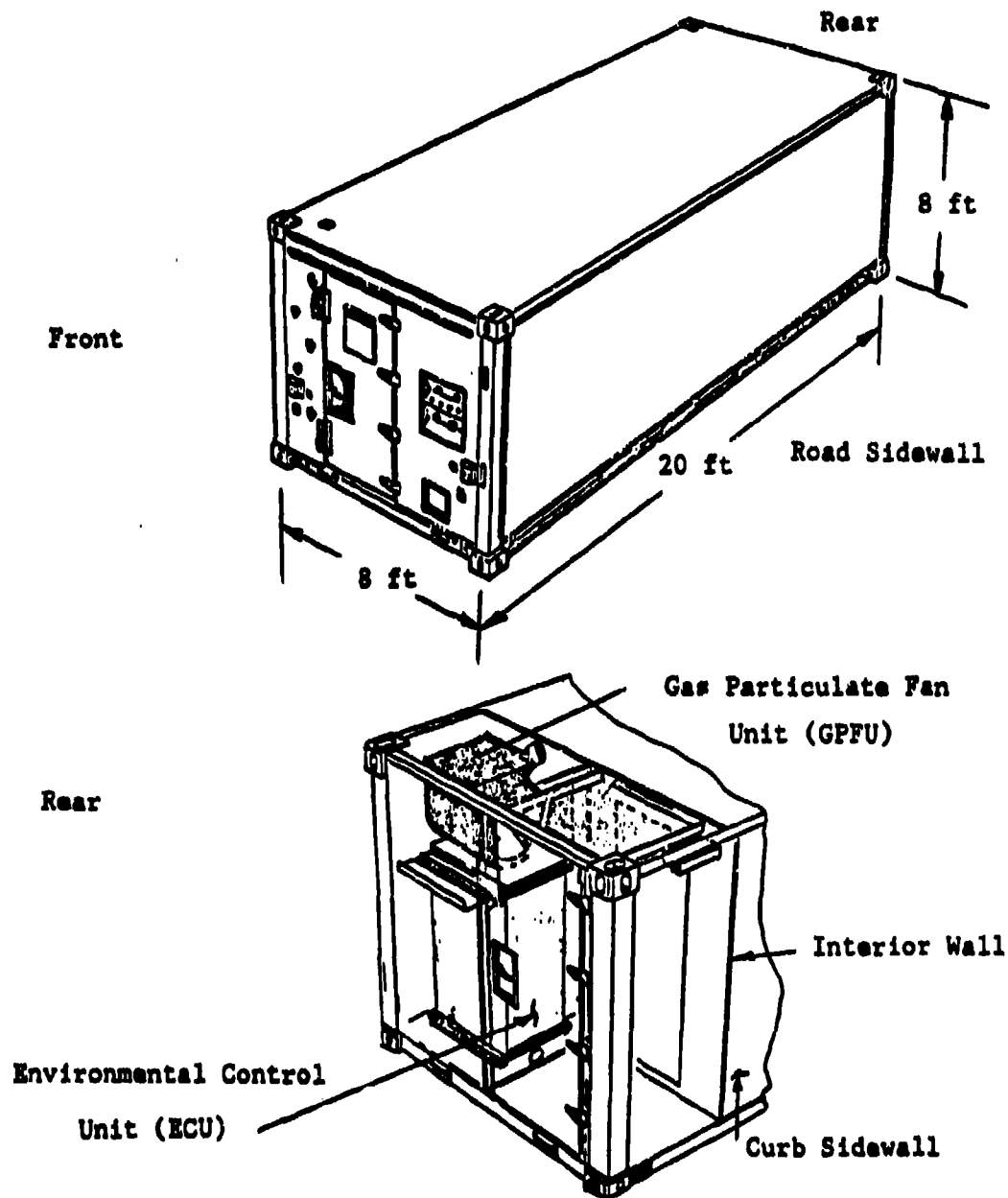


Figure 3. Front and rear ends of shelter, Gas Particulate Fan Unit (GPFU) and Environmental Control Unit (ECU).

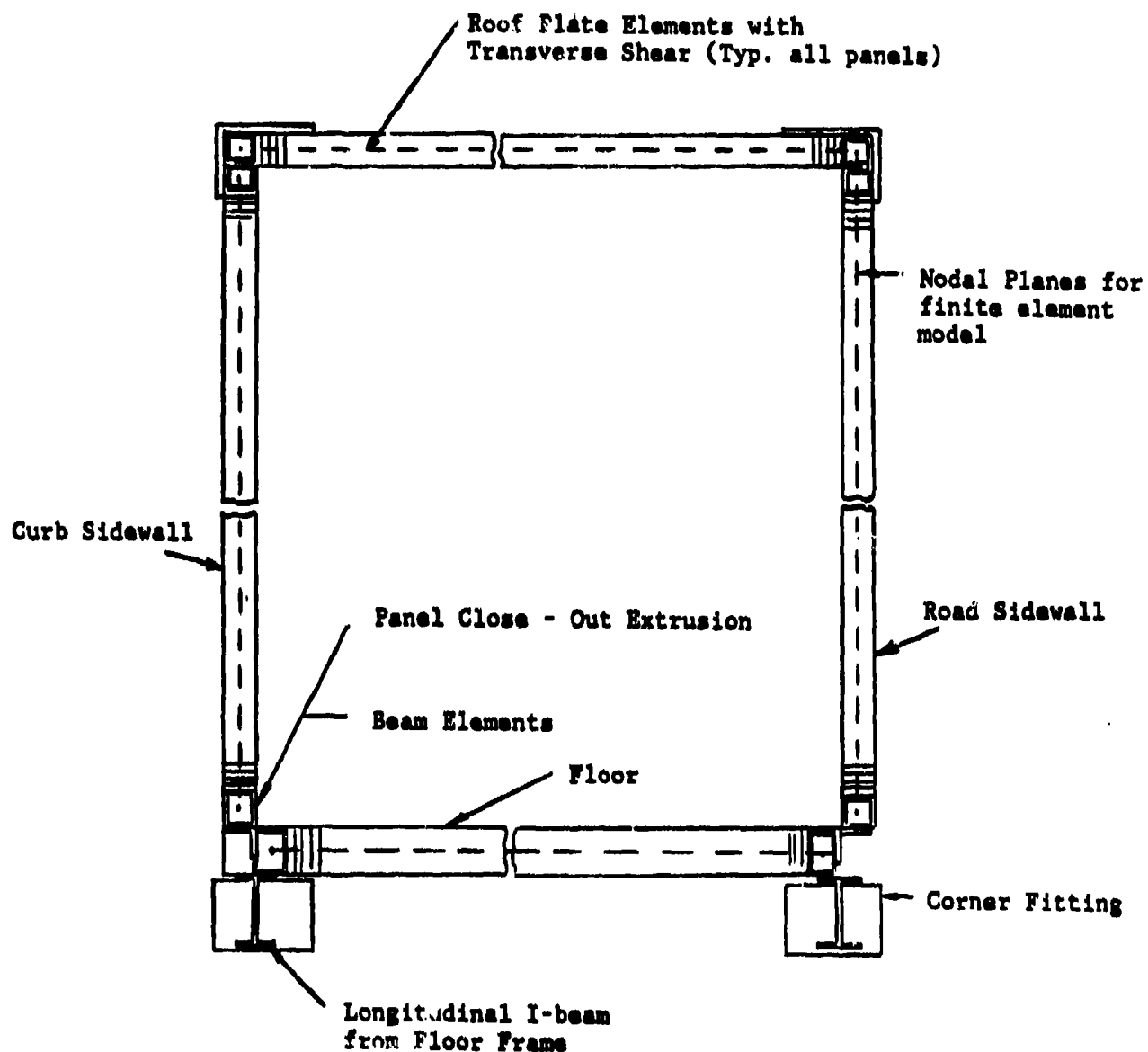


Figure 4. Transverse cross sectional view of shelter.

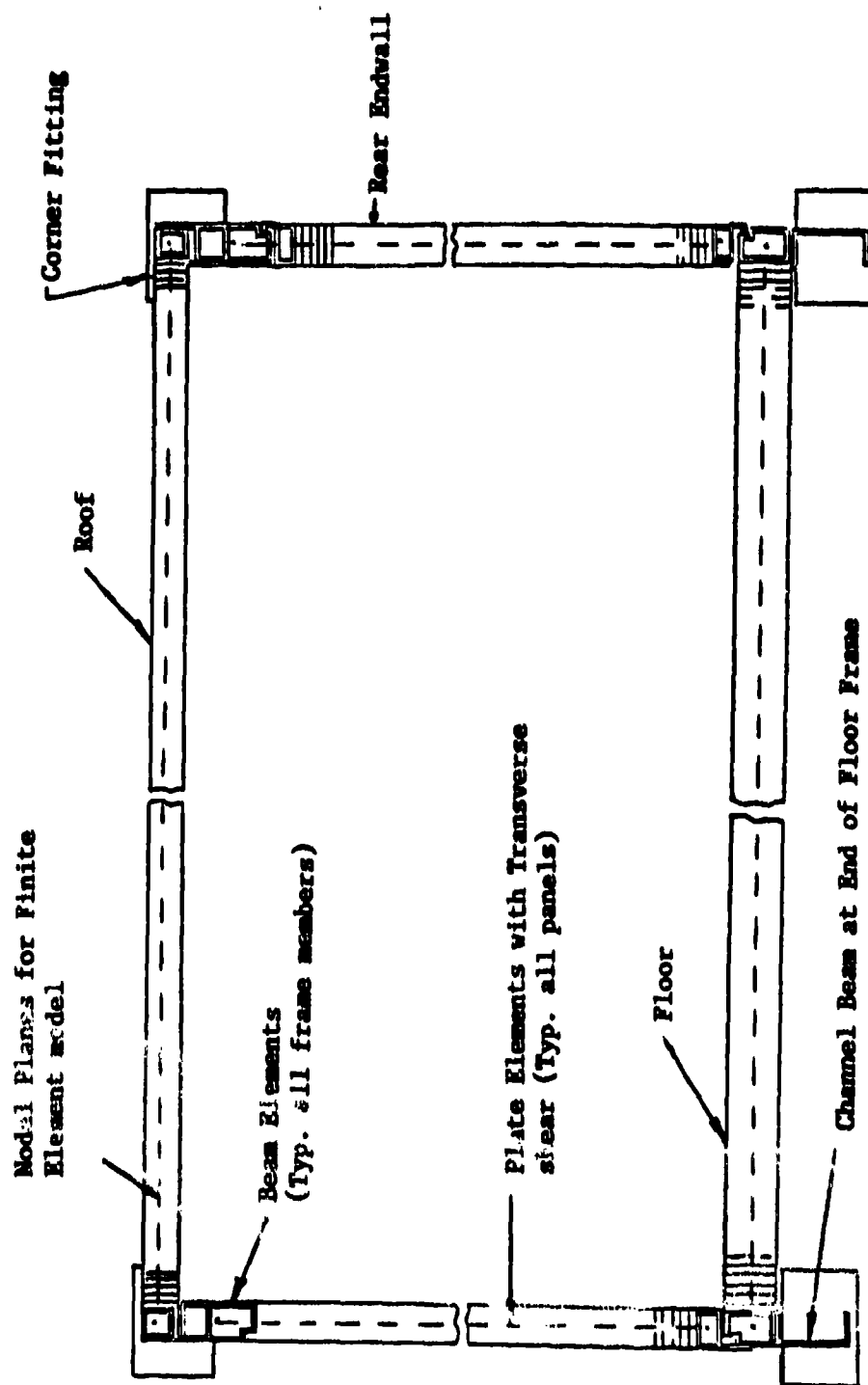


Figure 5. Longitudinal cross sectional view of shelter.

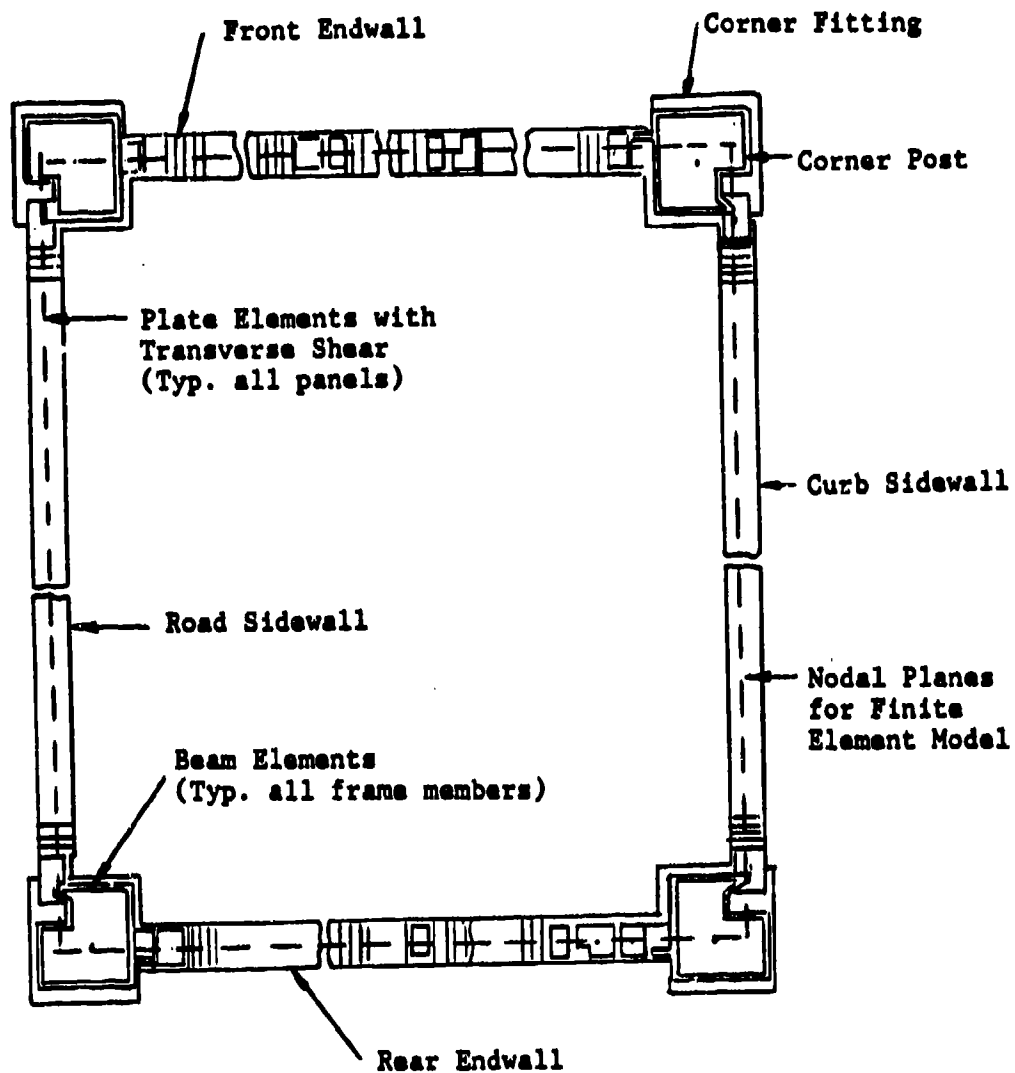
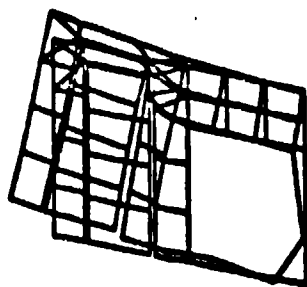


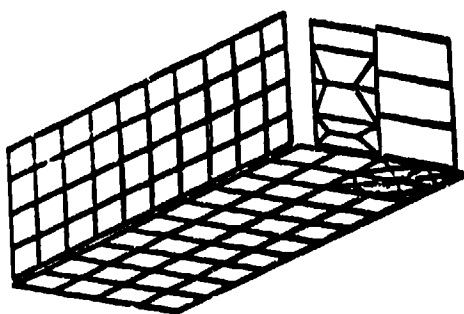
Figure 6. Plan cross sectional view of shelter.



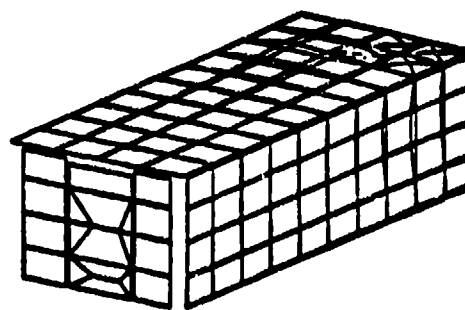
PROTECTIVE ENTRANCE
WALL



EQUIPMENT ROOM
WALL

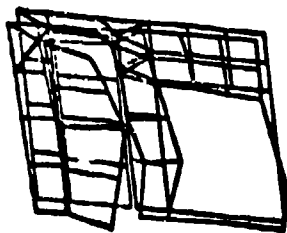


REAR ENDWALL, FLOOR,
CURB SIDEWALL

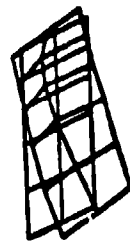


FRONT ENDWALL, ROOF
ROAD SIDEWALL

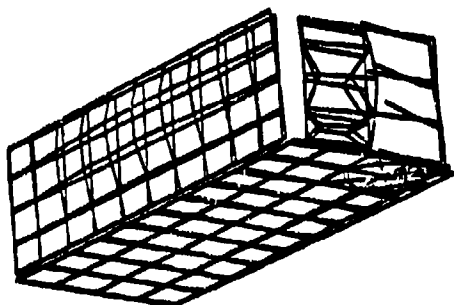
Figure 7. Free body mode shape for $f = 34.149$ Hz.



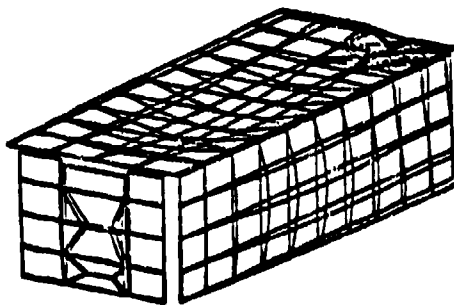
PROTECTIVE ENTRANCE
WALL



EQUIPMENT ROOM
WALL

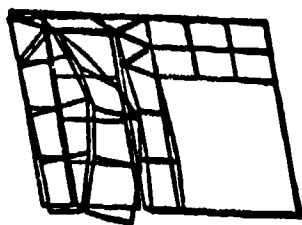


REAR ENDWALL, FLOOR,
CURB SIDEWALL



FRONT ENDWALL, ROOF
ROAD SIDEWALL

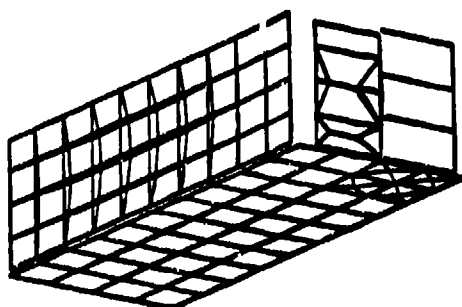
Figure 8. Free body mode shape for $f = 45.825$ Hz.



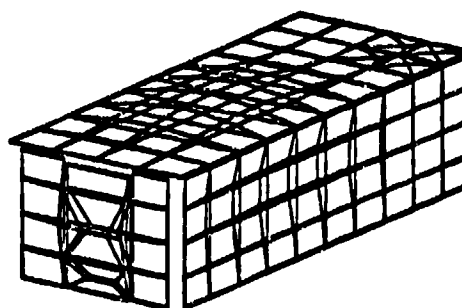
PROTECTIVE ENTRANCE
WALL



EQUIPMENT ROOM
WALL

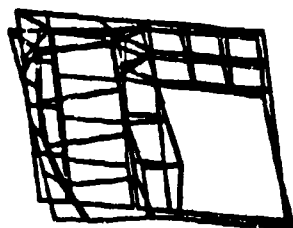


REAR ENDWALL, FLOOR,
CURB SIDEWALL

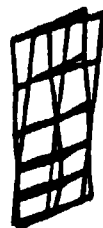


FRONT ENDWALL, ROOF
ROAD SIDEWALL

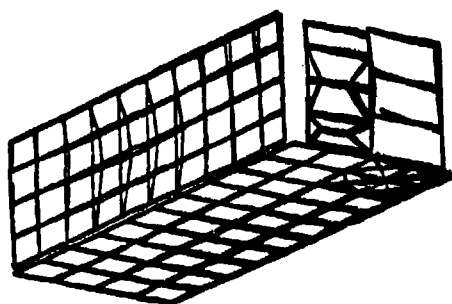
Figure 9. Free body mode shape for $f = 48.587$ Hz.



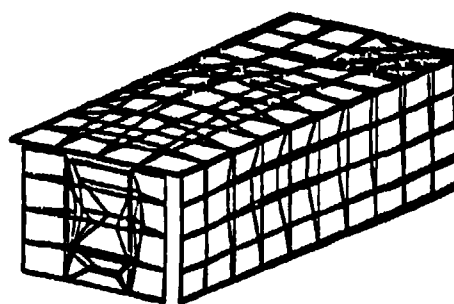
PROTECTIVE ENTRANCE
WALL



EQUIPMENT ROOM
WALL

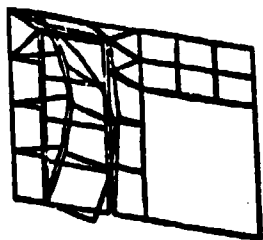


REAR ENDWALL, FLOOR,
CURB SIDEWALL



FRONT ENDWALL, ROOF
ROAD SIDEWALL

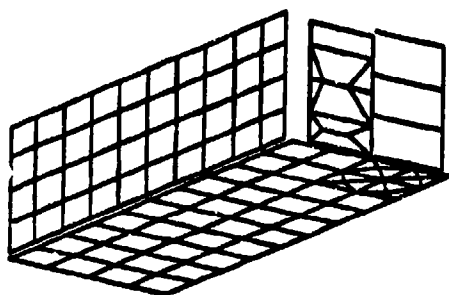
Figure 10. Free body mode shape for $f = 49.139$ Hz.



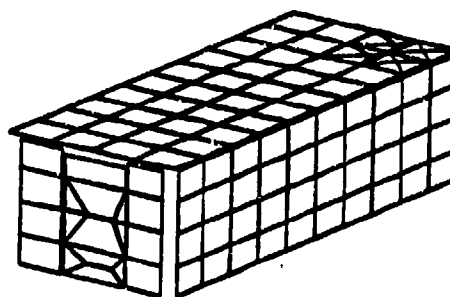
PROTECTIVE ENTRANCE
WALL



EQUIPMENT ROOM
WALL

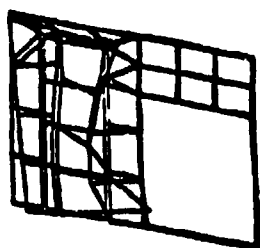


REAR ENDWALL, FLOOR,
CURB SIDEWALL



FRONT ENDWALL, ROOF
ROAD SIDEWALL

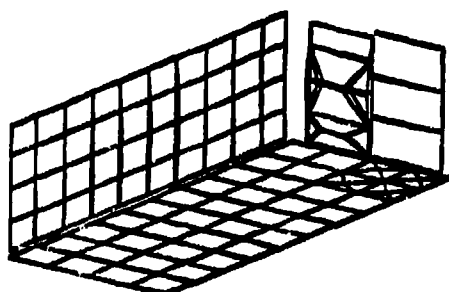
Figure 11. Free body mode shape for $f = 49.987$ Hz.



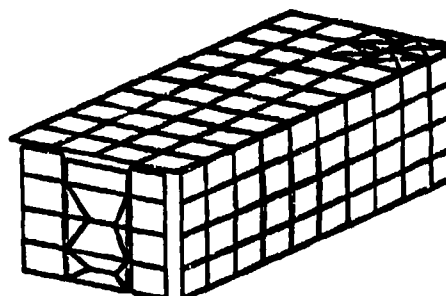
PROTECTIVE ENTRANCE
WALL



EQUIPMENT ROOM
WALL

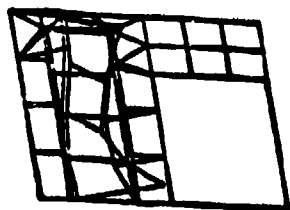


REAR ENDWALL, FLOOR,
CURB SIDEWALL

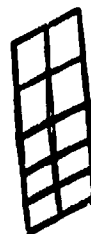


FRONT ENDWALL, ROOF
ROAD SIDEWALL

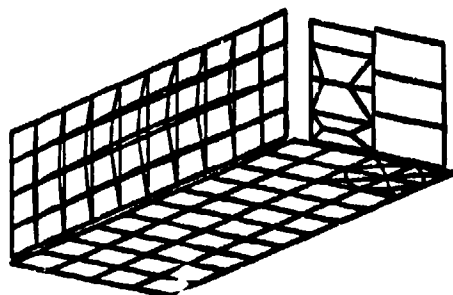
Figure 12. Free body mode shape for $f = 64.049$ Hz.



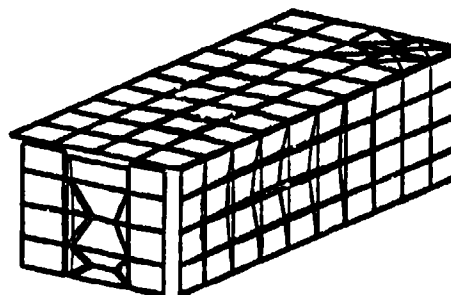
PROTECTIVE ENTRANCE
WALL



EQUIPMENT ROOM
WALL

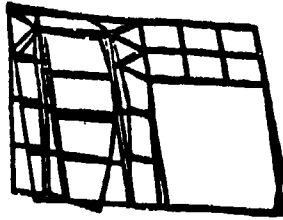


REAR ENDWALL, FLOOR,
CURB SIDEWALL



FRONT ENDWALL, ROOF
ROAD SIDEWALL

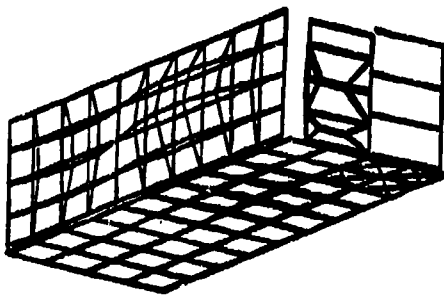
Figure 13. Free body mode shape for $f = 67.244$ Hz.



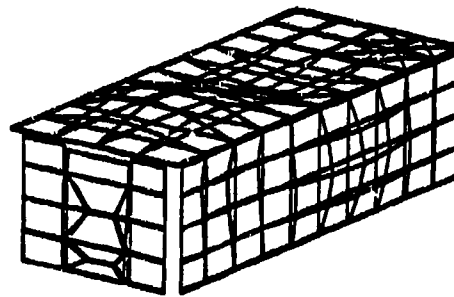
PROTECTIVE ENTRANCE
WALL



EQUIPMENT ROOM
WALL

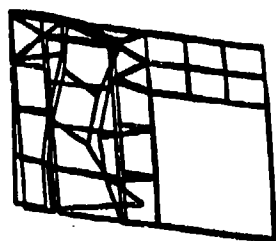


REAR ENDWALL, FLOOR,
CURB SIDEWALL



FRONT ENDWALL, ROOF
ROAD SIDEWALL

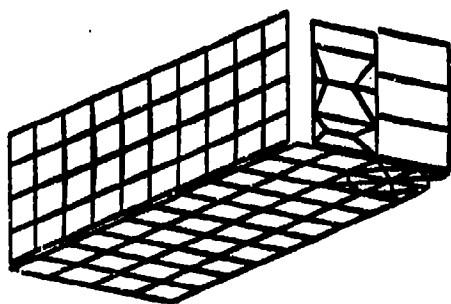
Figure 14. Free body mode shape for $f = 67.497$ Hz.



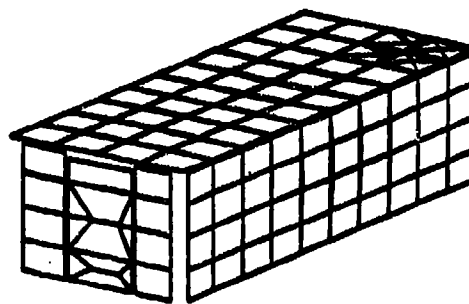
PROTECTIVE ENTRANCE
WALL



EQUIPMENT ROOM
WALL

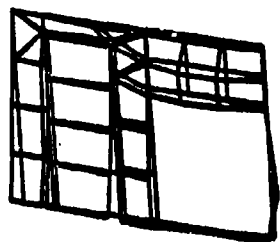


REAR ENDWALL, FLOOR,
CURB SIDEWALL



FRONT ENDWALL, ROOF
ROAD SIDEWALL

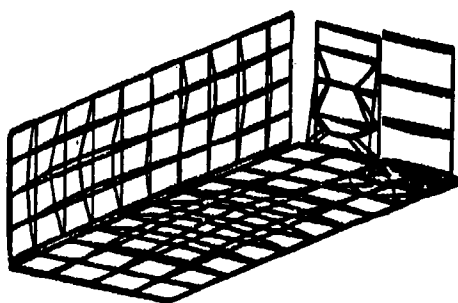
Figure 15. Free body mode shape for $f = 69.188$ Hz.



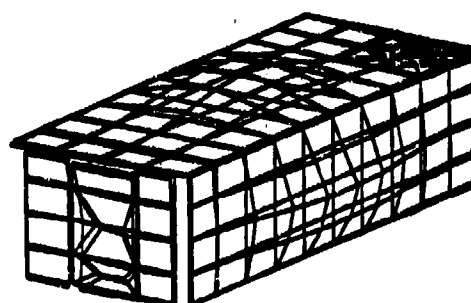
PROTECTIVE ENTRANCE
WALL



EQUIPMENT ROOM
WALL



REAR ENDWALL, FLOOR,
CURB SIDEWALL



FRONT ENDWALL, ROOF
ROAD SIDEWALL

Figure 16. Free body mode shape for $f = 71.771$ Hz.

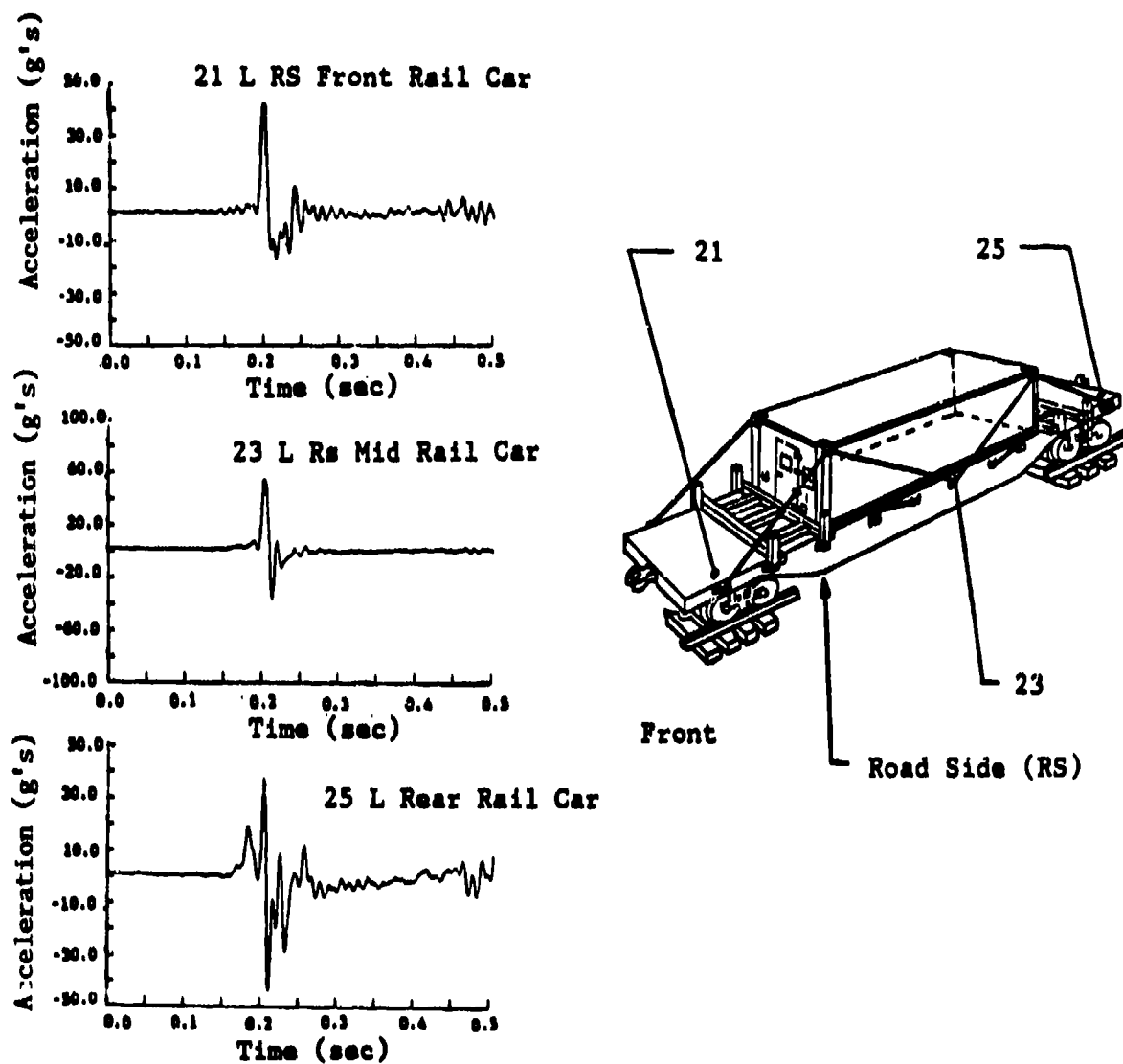


Figure 17. Longitudinal acceleration profiles along road side of rail car.

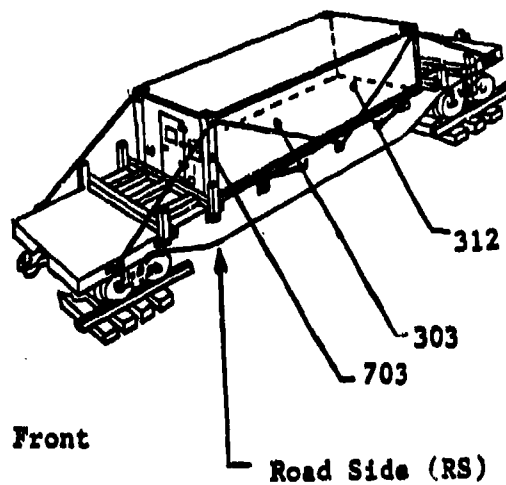
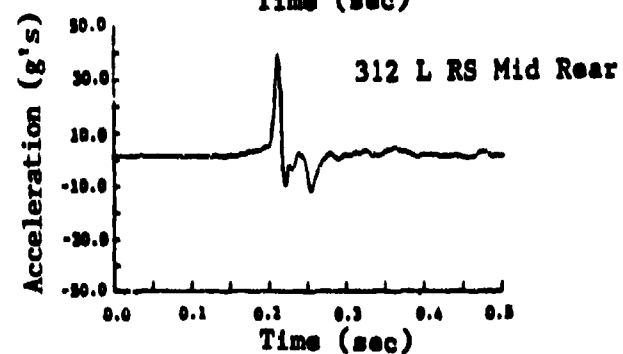
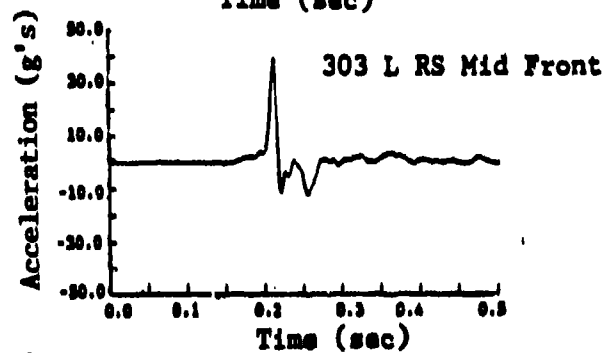
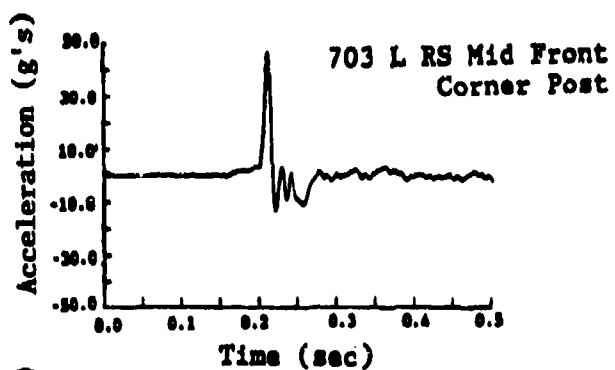


Figure 18. Longitudinal accelerations along road side wall at midheight.

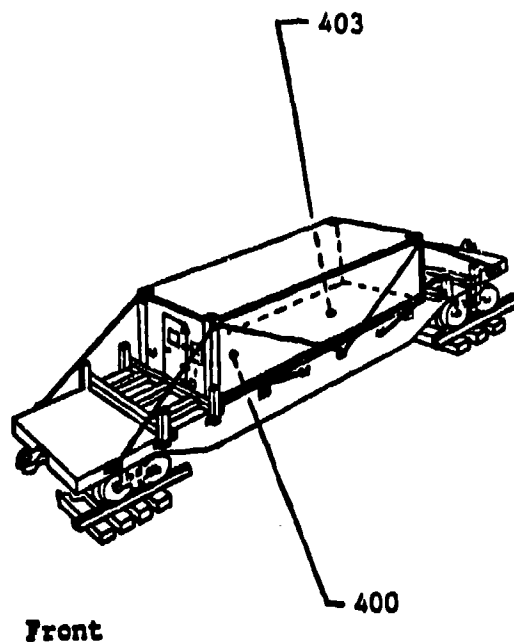
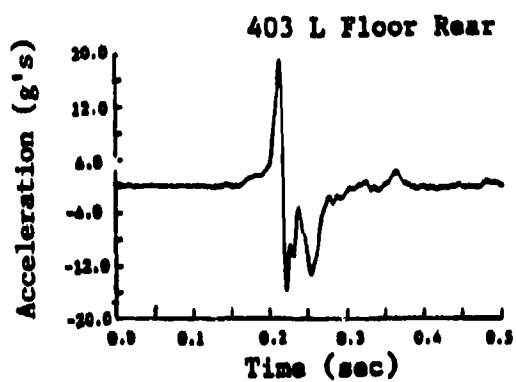
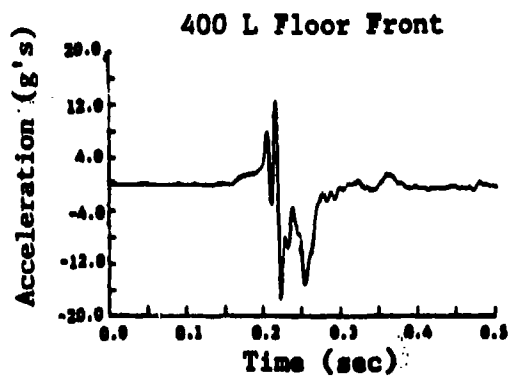
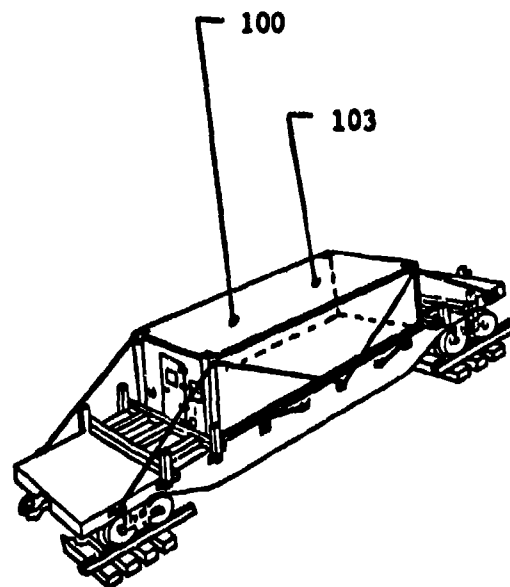
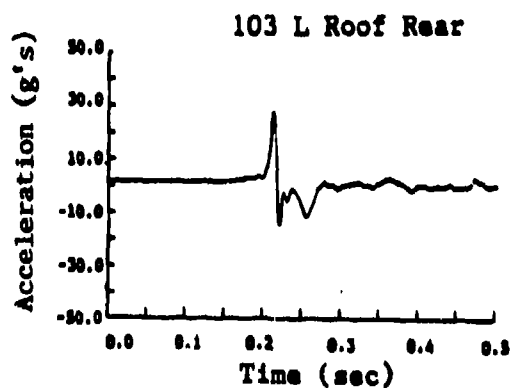
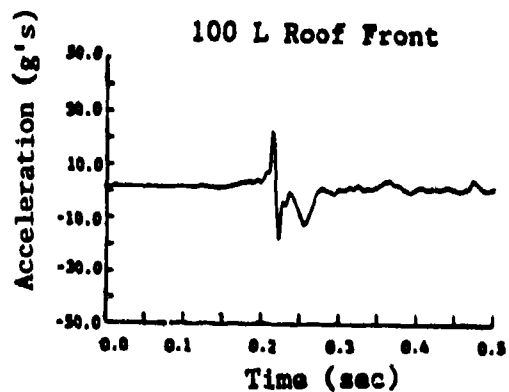


Figure 19. Longitudinal accelerations along longitudinal centerline of floor.



Front

Figure 20. Longitudinal accelerations along longitudinal centerline of roof.

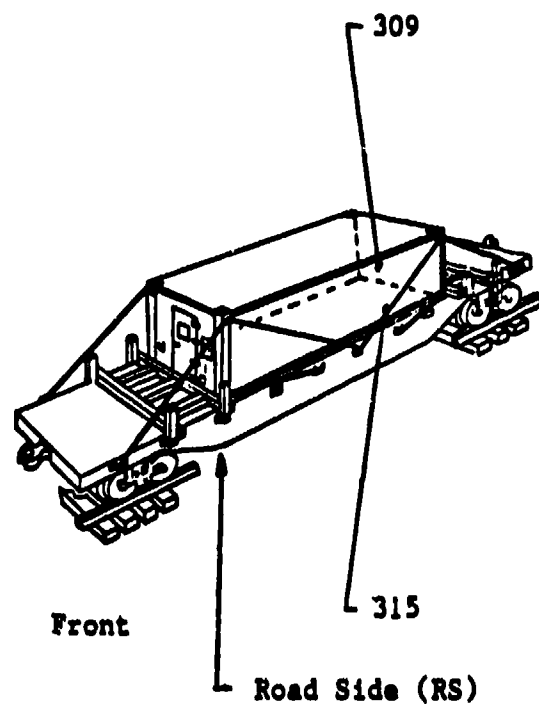
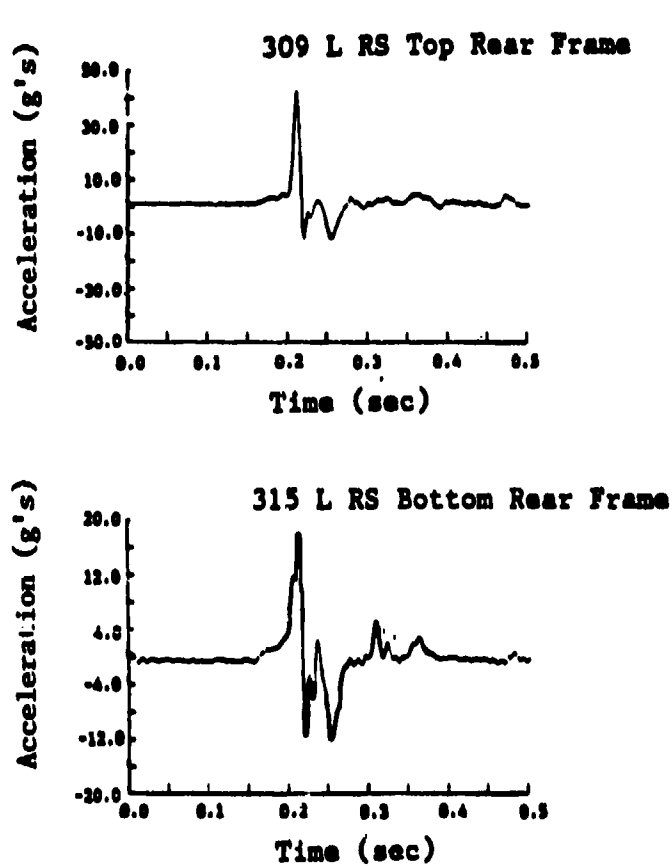


Figure 21. Longitudinal accelerations at bottom and top of road side wall near rear of shelter.

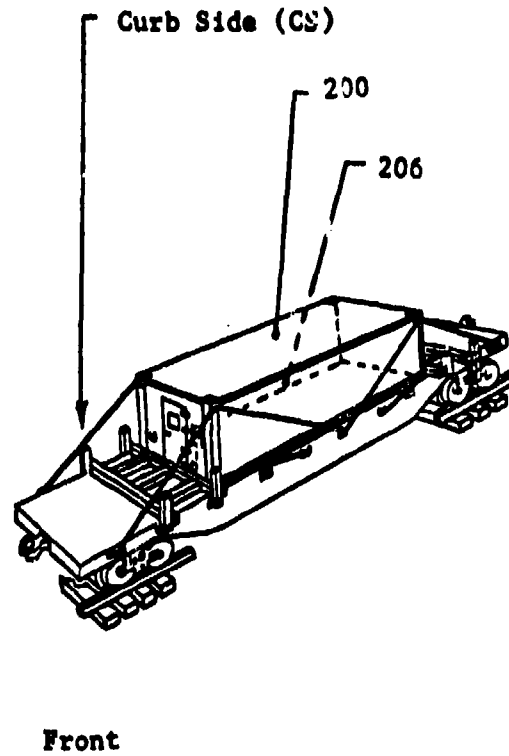
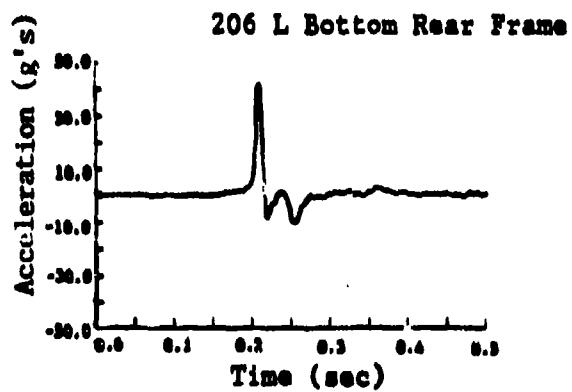
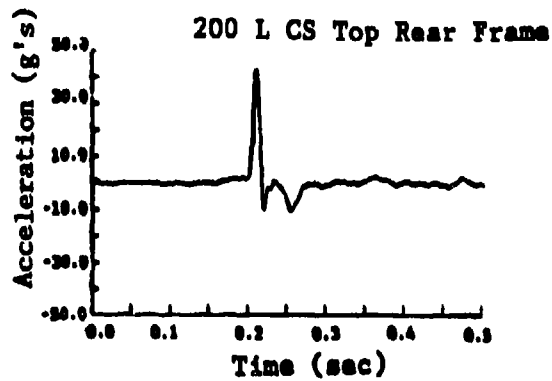


Figure 22. Longitudinal accelerations at bottom and top of curb side wall near rear of shelter.

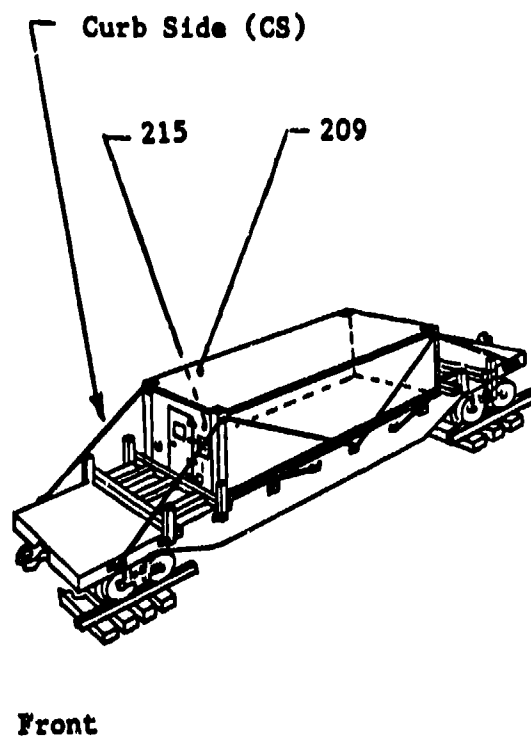
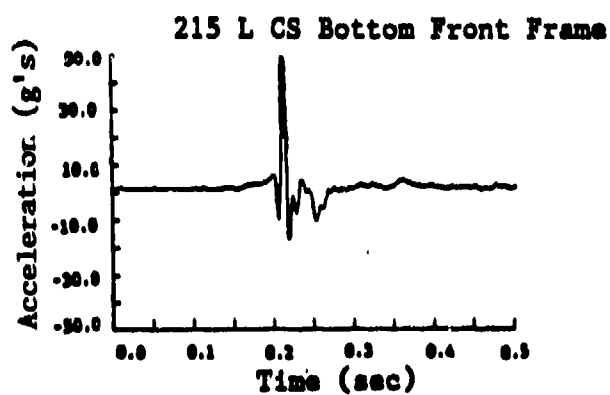
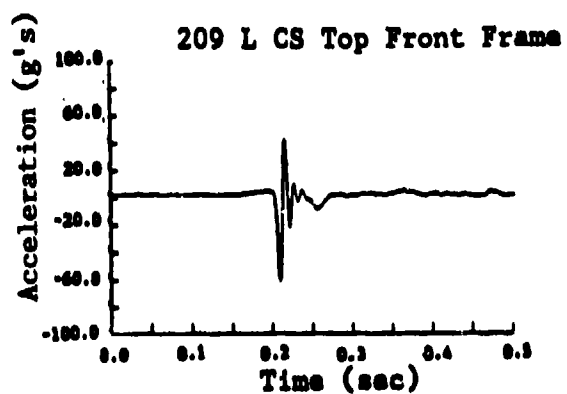


Figure 23. Longitudinal accelerations at bottom and top of curb side wall near front of shelter.

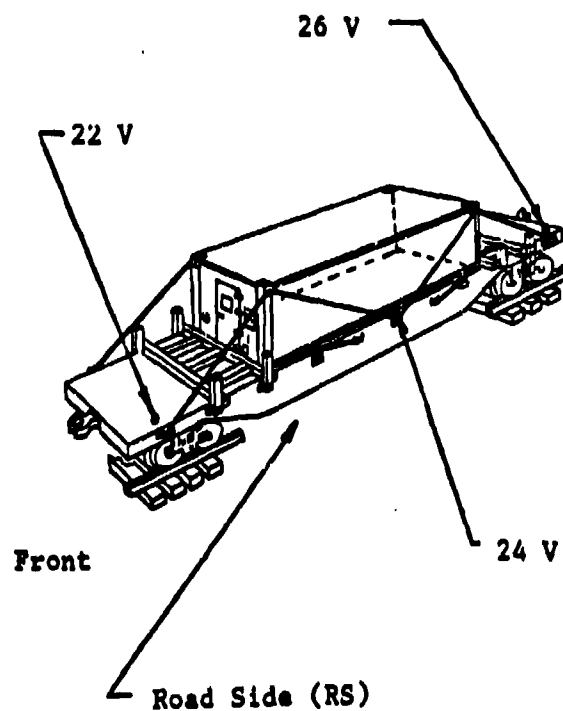
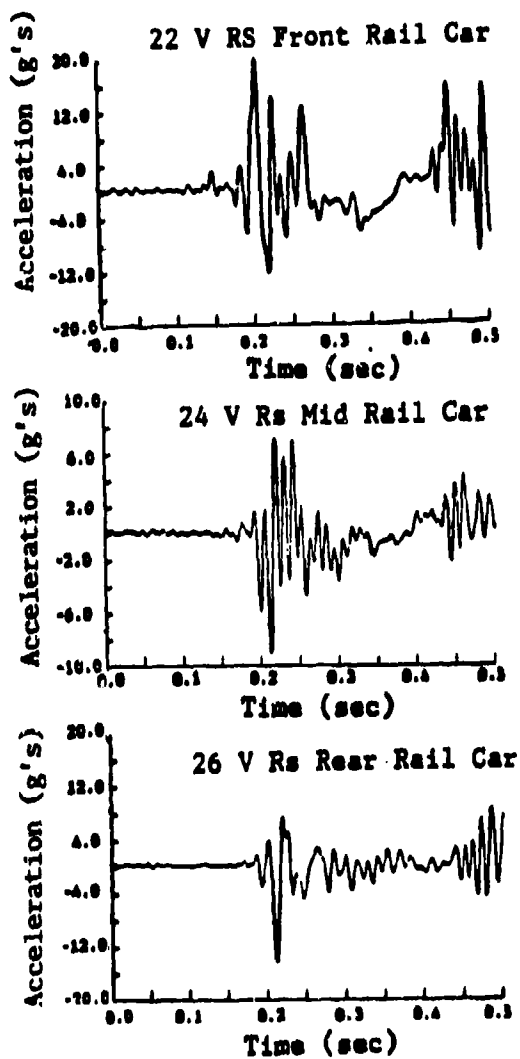


Figure 24. Vertical accelerations along road side of rail car.

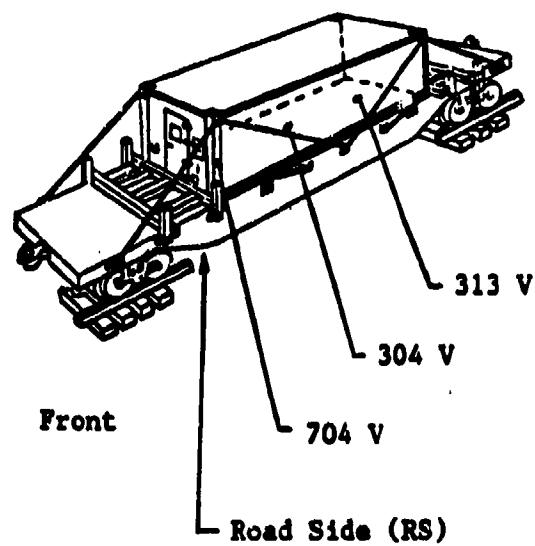
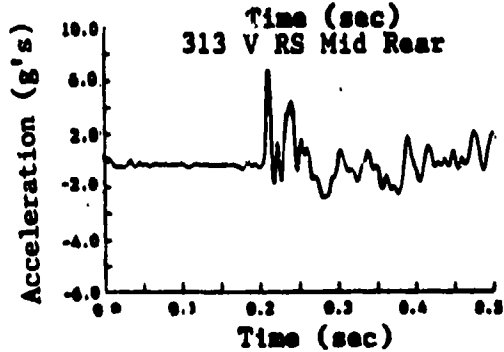
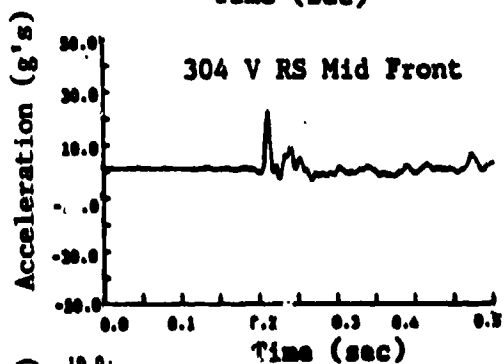
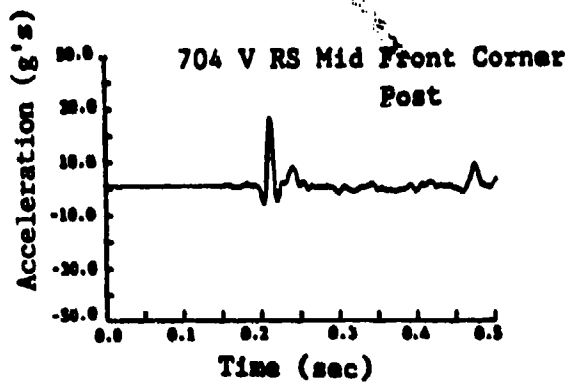


Figure 25. Vertical accelerations along road side wall at midheight.

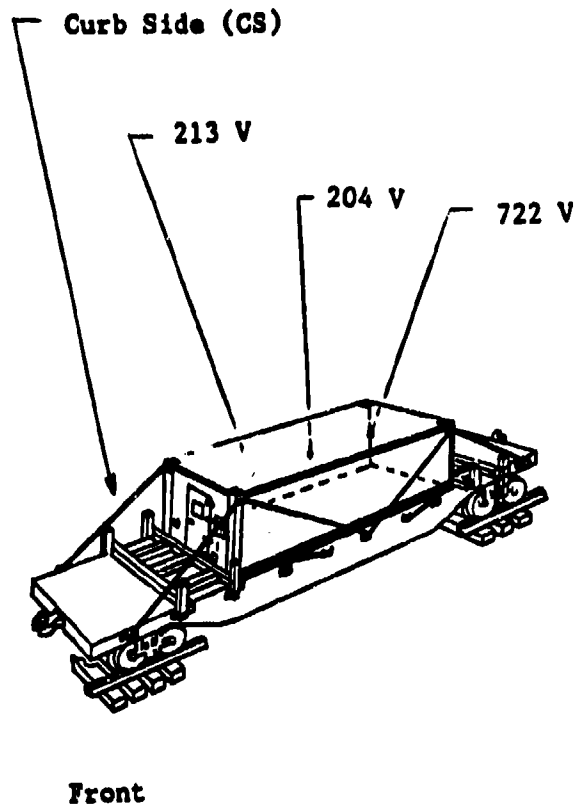
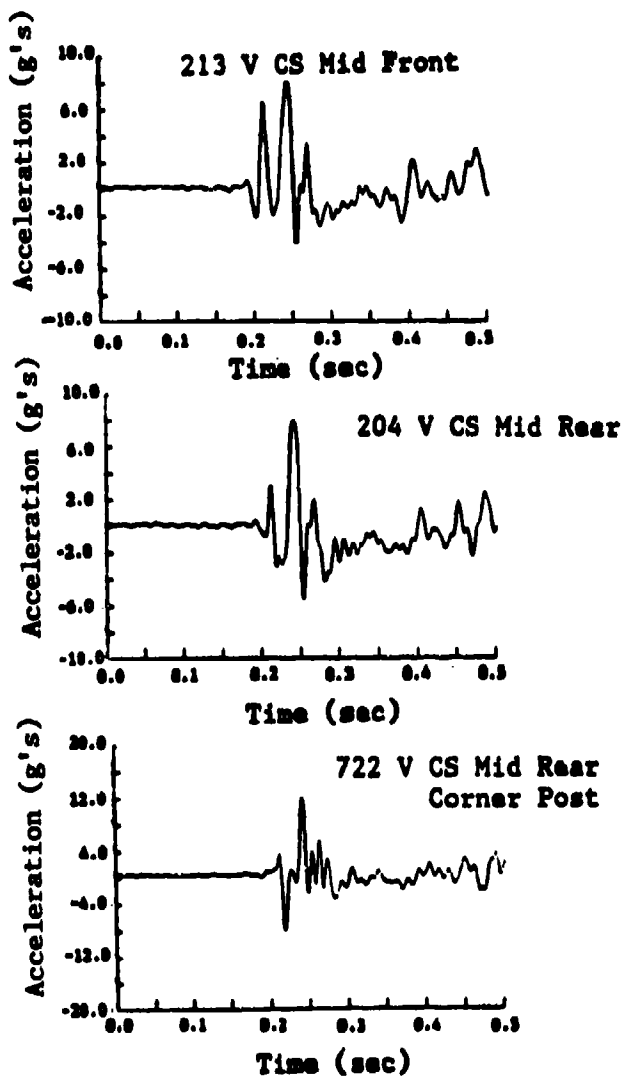


Figure 26. Vertical accelerations along curb side wall at midheight.

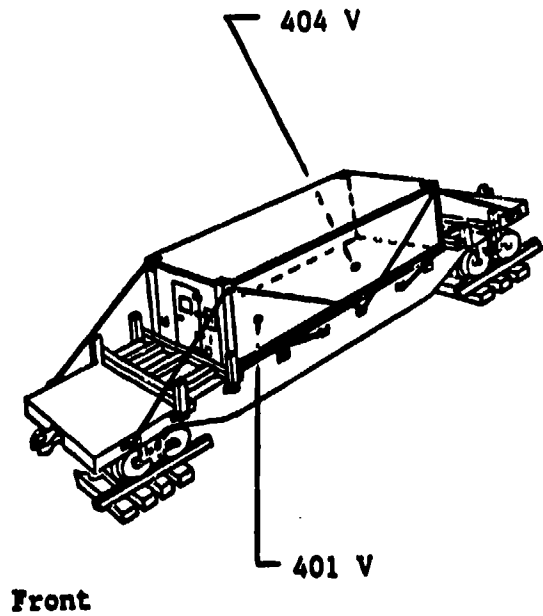
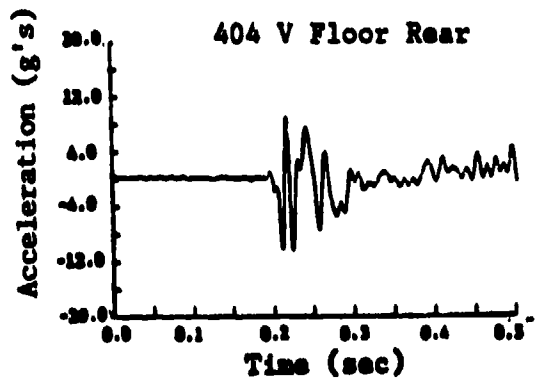
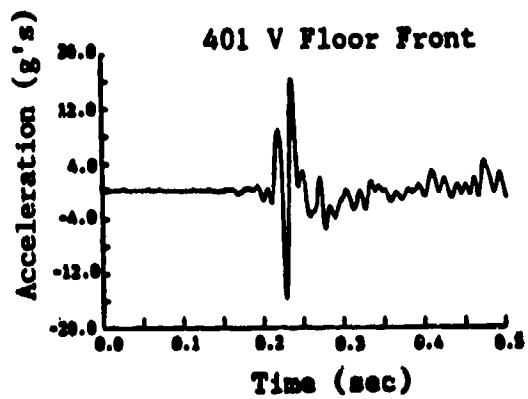


Figure 27. Vertical accelerations along longitudinal centerline of floor.

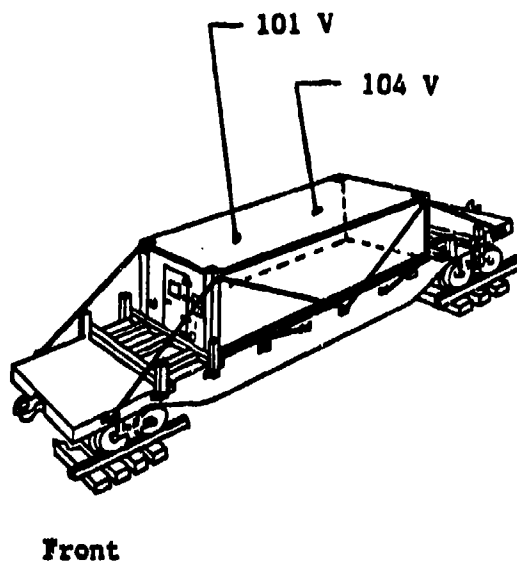
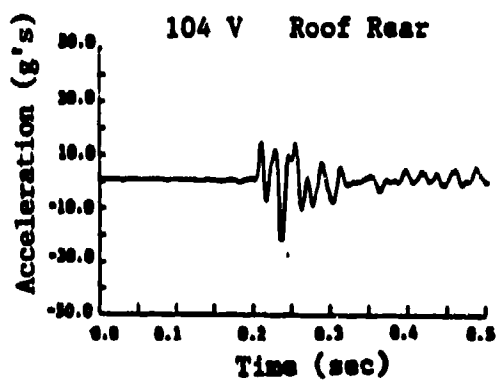
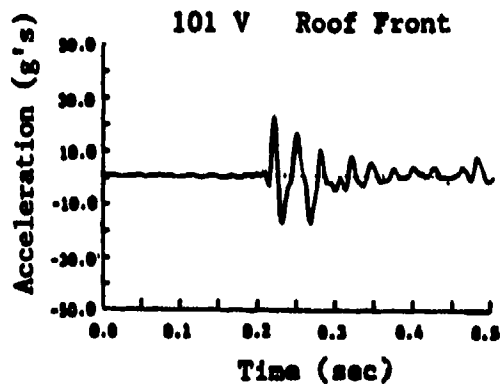


Figure 28. Vertical accelerations along longitudinal centerline of roof.

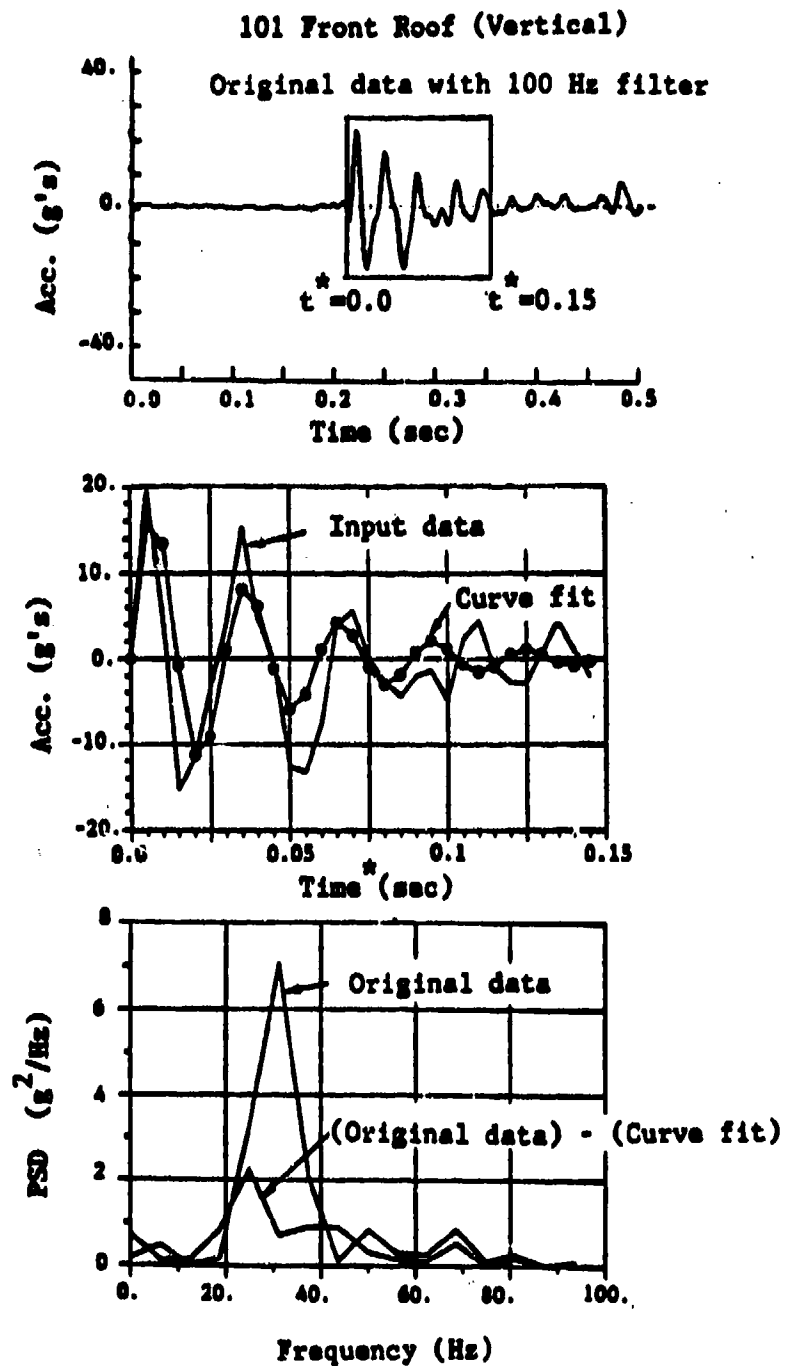


Figure 29. Vertical acceleration near front longitudinal center of roof, curve fit to data, power spectral density curves.

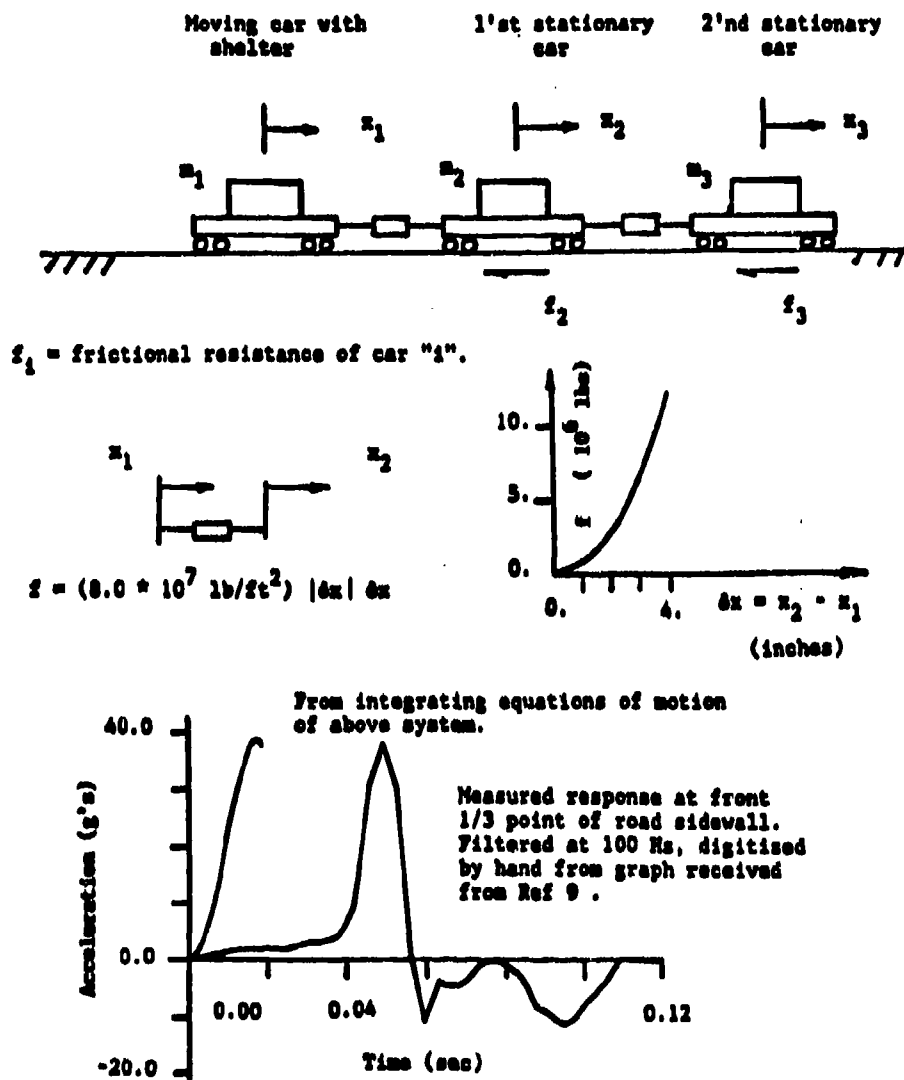
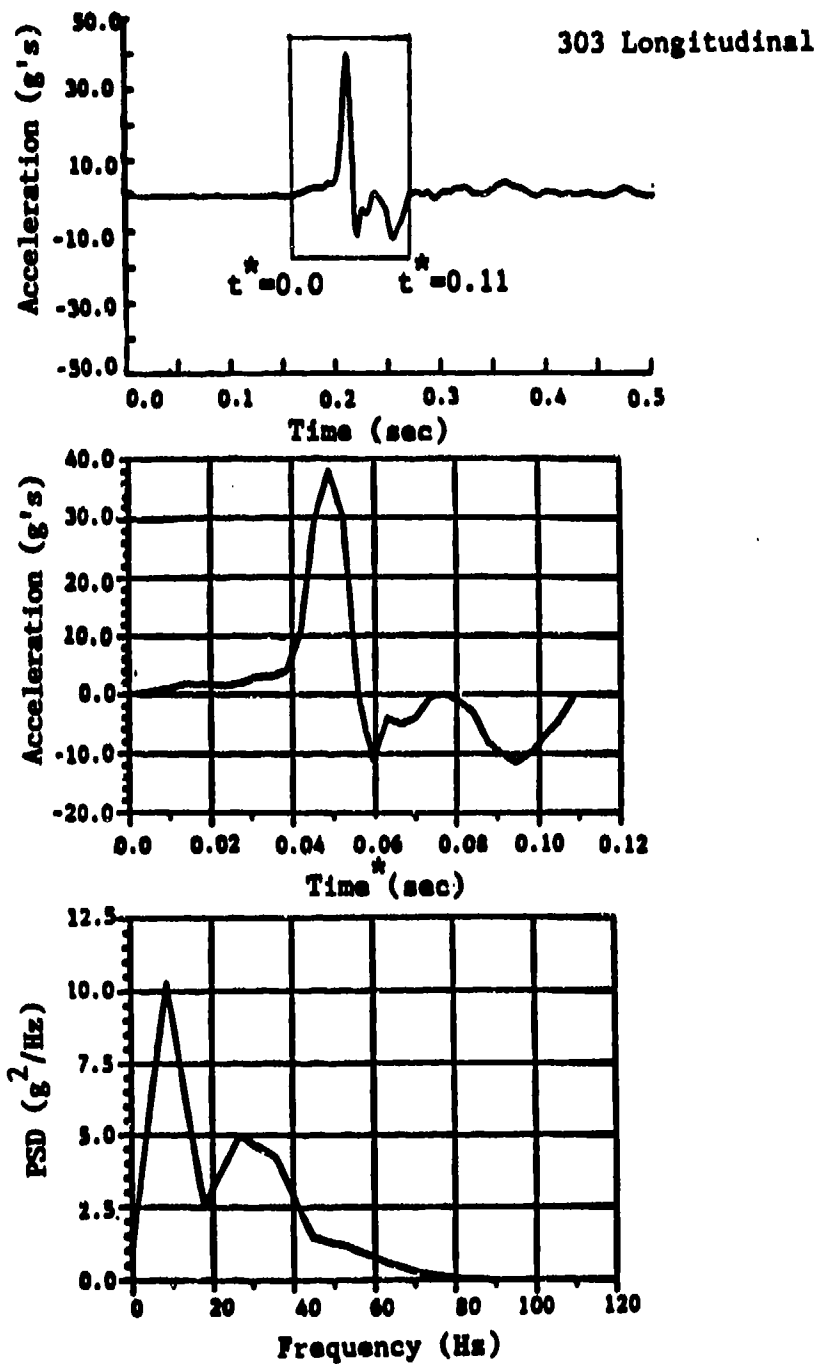


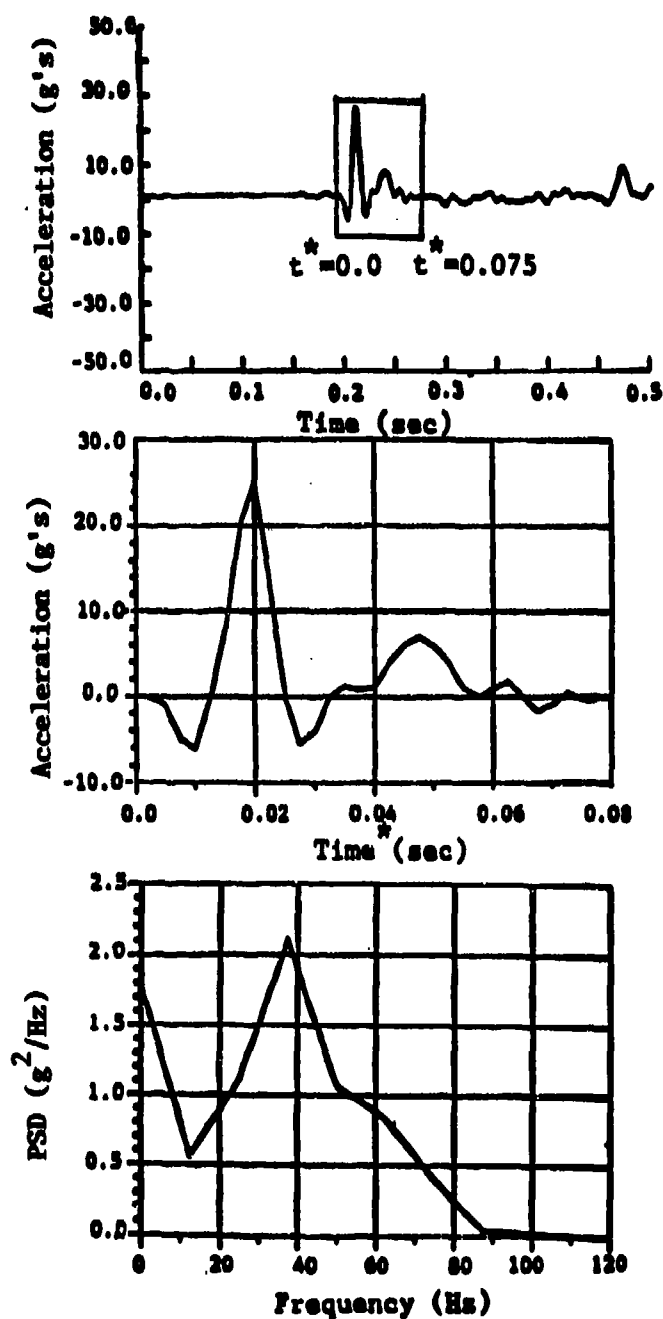
Figure 30. Model of rail cars during impact, nonlinear coupler, and shapes of acceleration curves for measured and computed data.



Accelerometer Location: Mid-Front Road Sidewall

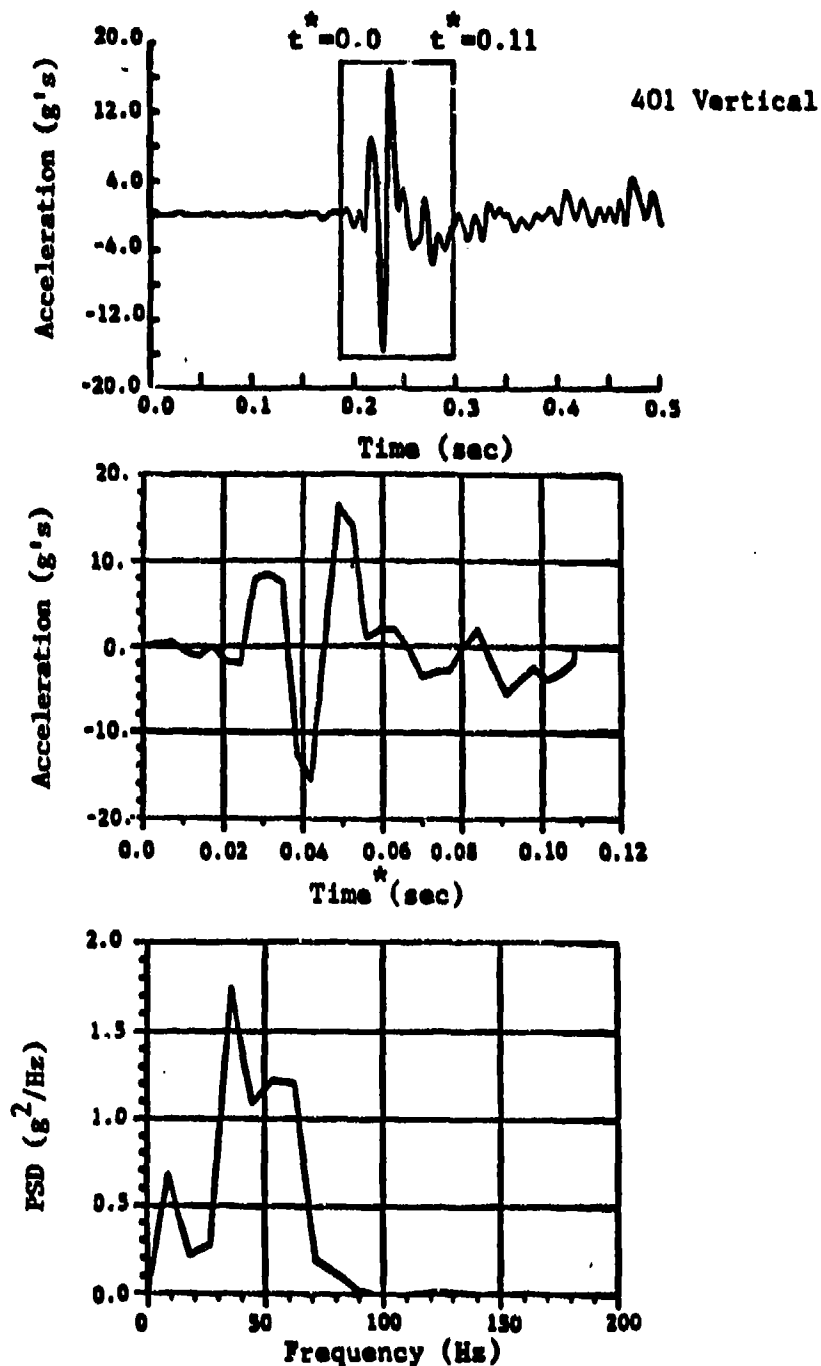
Figure 31. Midfront road side wall longitudinal acceleration and PSD curves for 100 Hz filtered data.

704 Vertical



Accelerometer Location: middle of road sidewall
front corner post

Figure 32. Midfront road side corner post vertical acceleration and PSD curves for 100 Hz filtered data.



Accelerometer Location: Mid-Front Floor

Figure 33. Midfront floor vertical acceleration and PSD curves for 100 Hz filtered data.

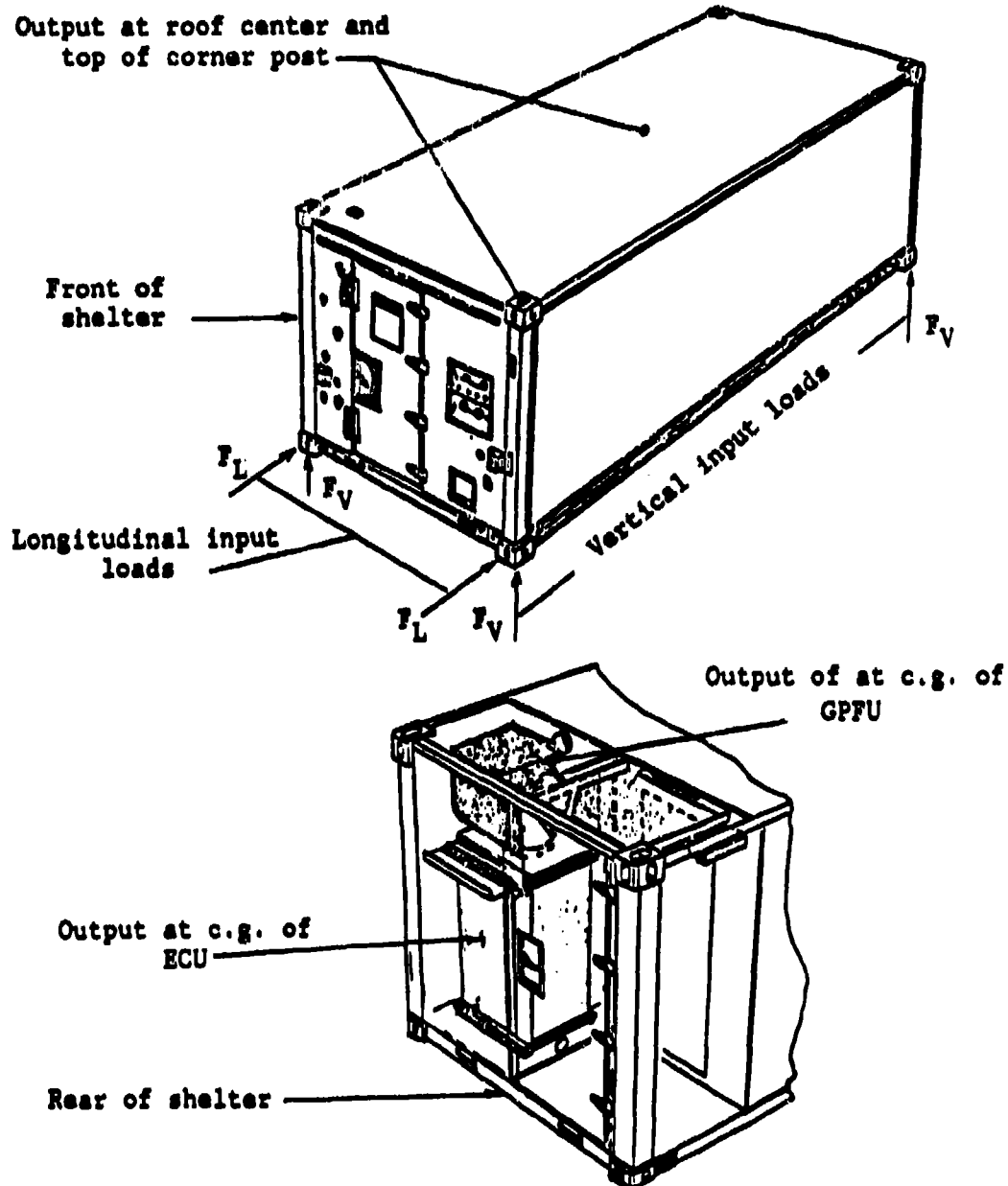


Figure 34. Locations on shelter for application of impulse loads and output locations.

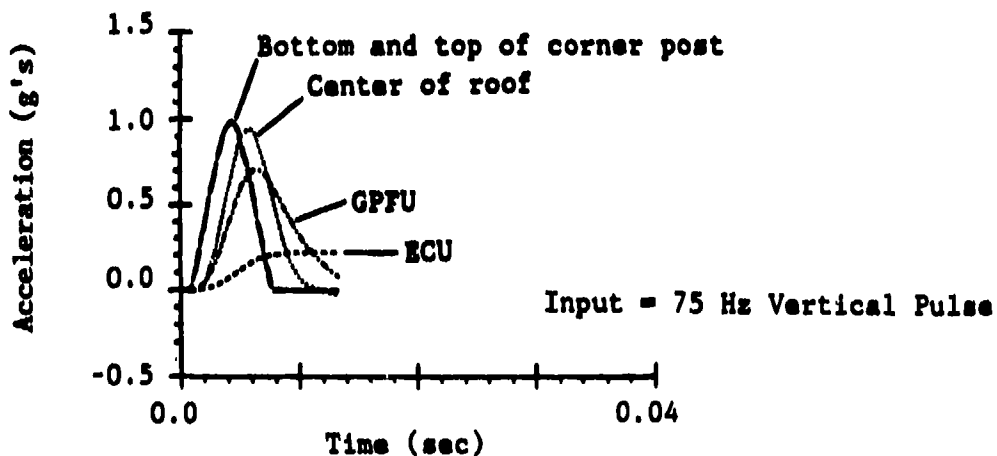
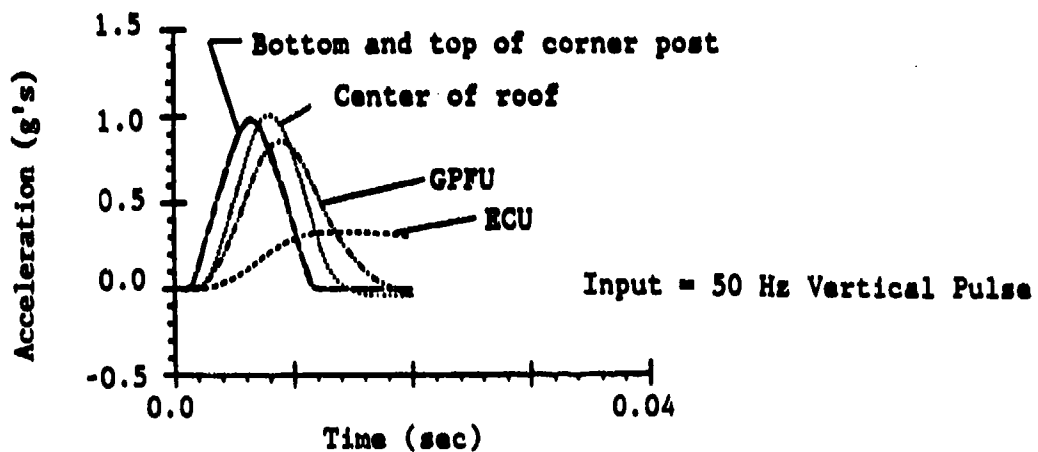
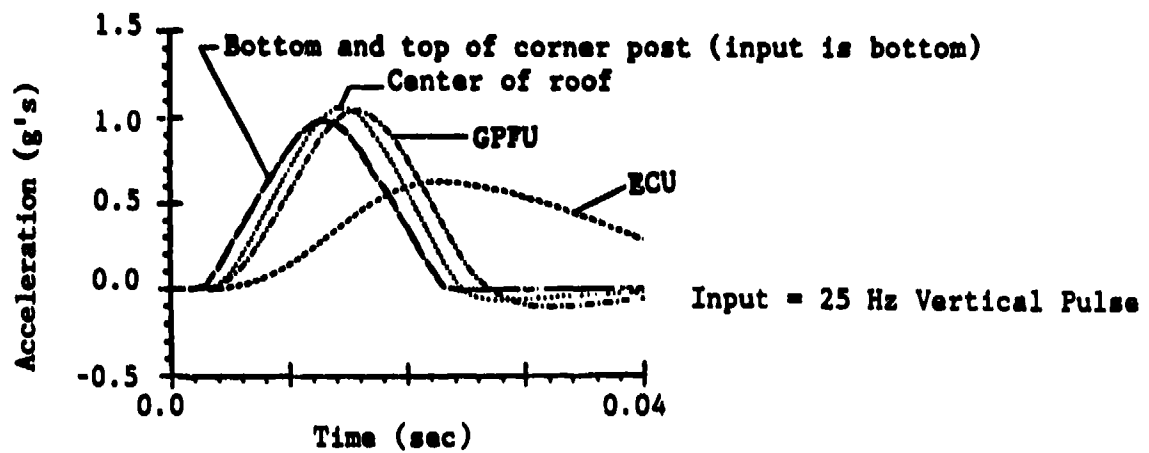


Figure 35. Vertical acceleration profiles for 25, 50 and 75 Hz vertical acceleration pulses applied to all bottom corner fittings.

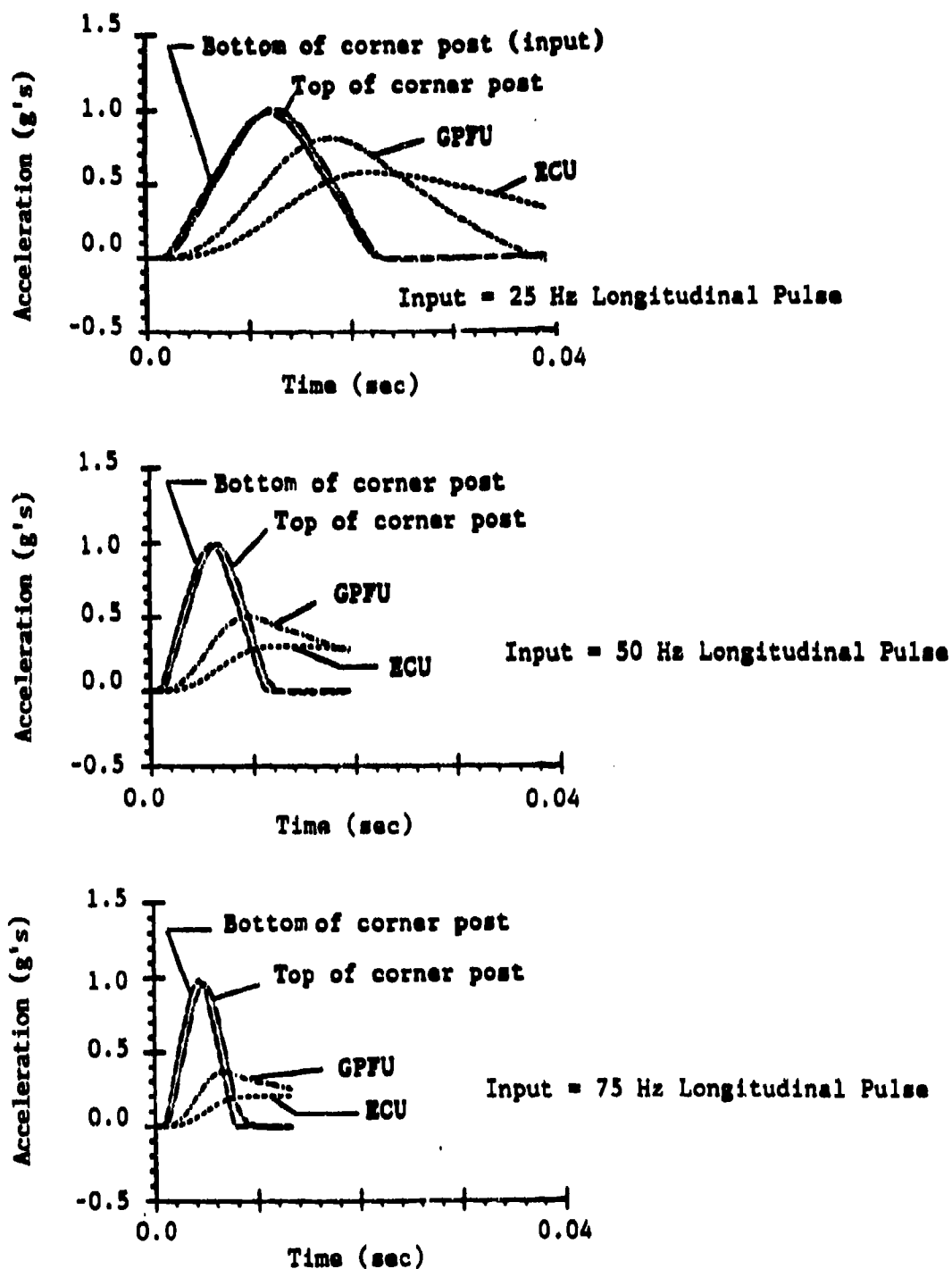


Figure 36. Longitudinal acceleration profiles for 25, 50 and 75 Hz longitudinal acceleration pulses applied to front bottom corner fittings.

DISTRIBUTION LIST

No. of Copies	To
1	Office of the Under Secretary of Defense for Research and Engineering, The Pentagon, Washington, DC 20301
	Commander, U.S. Army Laboratory Command, 2800 Powder Mill Road, Adelphi, MD 20783-1145
1	ATTN: SLCIS-IM-TL
2	Commander, Defense Technical Information Center, Cameron Station, Building 5, 5010 Duke Street, Alexandria, VA 22314
	Commander, Army Research Office, P.O. Box 12211, Research Triangle Park, NC 27709
1	ATTN: Information Processing Office
1	Dr. Gary Anderson, Eng. Sci. Div.
	Commander, U.S. Army Materiel Command, 5001 Eisenhower Avenue, Alexandria, VA 22333
1	ATTN: AMCLD
	Commander, U.S. Army Belvoir R&D Center, Fort Belvoir, VA 22060
1	ATTN: STRBE-GE, D. Frink
	Commander, U.S. Army Communications Electronics Command, Fort Monmouth, NJ 07703
1	ATTN: AMSEL-ED
1	AMSEL-ATDD
	Commander, U.S. Army Electronics Research and Development Command, Fort Monmouth, NJ 07703-5301
1	ATTN: DELSD-L (Reports Section)
1	DELEW-E, W. S. McAfee
1	DELS-D-EI, J. Roma
	Commander, U.S. Army Harry Diamond Laboratories, 2800 Powder Mill Road, Adelphi, MD 20783
1	ATTN: Mr. James Gaul
1	DELHD-TA-L
1	DRXDO-TI/002
1	DRXDO-NP
1	DELHD-RBA/J. Rosado
	Commander, U.S. Army Missile Command, Redstone Arsenal, AL 35898
1	ATTN: AMSMI-RD
1	AIAMS-YDL
	Commander, U.S. Army Tank-Automotive Command, Warren, MI 48090
1	ATTN: AMSTA-TSL

No. of
Copies

To

1	Commander, Naval Electronic Systems Command, Washington, DC 20360 ATTN: PME 117-21A
1	Brunswick Corporation Defense Division, 325 Brunswick Lane, Marion, VA 24354 ATTN: R. McCord
1	D. Johnston
1	Craig Systems, 10 Industrial Way, Amesbury, MA 01913-4848 ATTN: T. L. Anderson
1	Gichner Mobile Systems, P.O. Box B, Dallastown, PA 17313 ATTN: W. E. Ciccarelli
1	Goodyear Aerospace Corp., Shelter Engineering Div., Litchfield, Park, AZ 85340 ATTN: R. M. Brown, Bldg. 1
1	Grumman Aircraft Division, MS B10-25, Bethpage, NY 11714 ATTN: Peter Shyprykevich
1	S. Dastin
1	Kaman AviDyne, 83 Second Ave., Northwest Industrial Park, Burlington, MA 01803 ATTN: R. Milligan
1	D. Coyne
1	Commander, U.S. Army Natick Research, Development and Engineering Center, Kansas Street, Natick, MA 01760 ATTN: E. Steeves, STRNC-UE
1	J. Calligeros, STRNC-UE
10	Tactical Shelters Branch, STRNC-UST
1	Director, U.S. Army Materials Technology Laboratory, Watertown, MA 02172-0001 ATTN: SLCMT-IML
2	Authors

U.S. Army Materials Technology Laboratory
Watertown, Massachusetts 02172-0001
DYNAMIC ANALYSIS OF A TACTICAL RIGID SHELTER
SUBJECTED TO RAIL IMPACT - Arthur R. Johnson
and James R. Cullinane

AD
UNCLASSIFIED
UNLIMITED DISTRIBUTION
Key Words

Technical Report MTL TR 86-45, December 1986, 50 pp -
Illius/Tables, ANCHS Code 643726-4280012,
D/A Project IE463720428

In this effort a technical database was developed for a Tactical Shelter experiencing rail impact. A finite element model of the shelter and internal equipment was made, a test was conducted in which accelerations were measured on the shelter, the flatcar, and on the internal equipment during rail impact. The measured accelerations on the flatcar were used to determine the spectra of the dynamic loads acting on the shelter and the response of the shelter to forced acceleration impulses in the frequency range of the measured data was determined. We found that the shelter's lowest structural vibration modes, as predicted by the finite element model, were in the range of the frequencies in the power spectral density representation of the rail car response. The shelter responded almost rigidly in the longitudinal direction but did vibrate in the vertical and transverse directions. Computed mode shapes, measured accelerations, analysis of the data and the predicted response of the shelter to impulse loadings are presented in the report.

U.S. Army Materials Technology Laboratory
Watertown, Massachusetts 02172-0001
DYNAMIC ANALYSIS OF A TACTICAL RIGID SHELTER
SUBJECTED TO RAIL IMPACT - Arthur R. Johnson
and James R. Cullinane

AD
UNCLASSIFIED
UNLIMITED DISTRIBUTION
Key Words

Technical Report MTL TR 86-45, December 1986, 50 pp -
Illius/Tables, ANCHS Code 643726-4280012,
D/A Project IE463720428

In this effort a technical database was developed for a Tactical Shelter experiencing rail impact. A finite element model of the shelter and internal equipment was made, a test was conducted in which accelerations were measured on the shelter, the flatcar, and on the internal equipment during rail impact. The measured accelerations on the flatcar were used to determine the spectra of the dynamic loads acting on the shelter and the response of the shelter to forced acceleration impulses in the frequency range of the measured data was determined. We found that the shelter's lowest structural vibration modes, as predicted by the finite element model, were in the range of the frequencies in the power spectral density representation of the rail car response. The shelter responded almost rigidly in the longitudinal direction but did vibrate in the vertical and transverse directions. Computed mode shapes, measured accelerations, analysis of the data and the predicted response of the shelter to impulse loadings are presented in the report.

U.S. Army Materials Technology Laboratory
Watertown, Massachusetts 02172-0001
DYNAMIC ANALYSIS OF A TACTICAL RIGID SHELTER
SUBJECTED TO RAIL IMPACT - Arthur R. Johnson
and James R. Cullinane

AD
UNCLASSIFIED
UNLIMITED DISTRIBUTION
Key Words

Technical Report MTL TR 86-45, December 1986, 50 pp -
Illius/Tables, ANCHS Code 643726-4280012,
D/A Project IE463720428

In this effort a technical database was developed for a Tactical Shelter experiencing rail impact. A finite element model of the shelter and internal equipment was made, a test was conducted in which accelerations were measured on the shelter, the flatcar, and on the internal equipment during rail impact. The measured accelerations on the flatcar were used to determine the spectra of the dynamic loads acting on the shelter and the response of the shelter to forced acceleration impulses in the frequency range of the measured data was determined. We found that the shelter's lowest structural vibration modes, as predicted by the finite element model, were in the range of the frequencies in the power spectral density representation of the rail car response. The shelter responded almost rigidly in the longitudinal direction but did vibrate in the vertical and transverse directions. Computed mode shapes, measured accelerations, analysis of the data and the predicted response of the shelter to impulse loadings are presented in the report.

U.S. Army Materials Technology Laboratory
Watertown, Massachusetts 02172-0001
DYNAMIC ANALYSIS OF A TACTICAL RIGID SHELTER
SUBJECTED TO RAIL IMPACT - Arthur R. Johnson
and James R. Cullinane

AD
UNCLASSIFIED
UNLIMITED DISTRIBUTION
Key Words

Technical Report MTL TR 86-45, December 1986, 50 pp -
Illius/Tables, ANCHS Code 643726-4280012,
D/A Project IE463720428

In this effort a technical database was developed for a Tactical Shelter experiencing rail impact. A finite element model of the shelter and internal equipment was made, a test was conducted in which accelerations were measured on the shelter, the flatcar, and on the internal equipment during rail impact. The measured accelerations on the flatcar were used to determine the spectra of the dynamic loads acting on the shelter and the response of the shelter to forced acceleration impulses in the frequency range of the measured data was determined. We found that the shelter's lowest structural vibration modes, as predicted by the finite element model, were in the range of the frequencies in the power spectral density representation of the rail car response. The shelter responded almost rigidly in the longitudinal direction but did vibrate in the vertical and transverse directions. Computed mode shapes, measured accelerations, analysis of the data and the predicted response of the shelter to impulse loadings are presented in the report.